DEMS Department of Economics, Management and Statistics

DEMS WORKING PAPER SERIES

Dynamic approaches for the evaluation of the environmental policy efficacy in a nonlinear Cournot duopoly with differentiated goods and emission charges

Ahmad Naimzada, Marina Pireddu

No. 517 – April 2023

Department of Economics, Management and Statistics
University of Milano – Bicocca
Piazza Ateneo Nuovo 1 – 2016 Milan, Italy
http://dems.unimib.it/

Dynamic approaches for the evaluation of the environmental policy efficacy in a nonlinear Cournot duopoly with differentiated goods and emission charges

Ahmad Naimzada [a*], Marina Pireddu [b†]

[a] Dept. of Economics, Management and Statistics, University of Milano - Bicocca,
U6 Building, Piazza dell'Ateneo Nuovo 1, 20126 Milano, Italy.

[b] Dept. of Mathematics and its Applications, University of Milano - Bicocca,
U5 Building, Via R. Cozzi 55, 20125 Milano, Italy.

Abstract

According to the existing empirical literature the price and the exchanged quantity volatility observed in real-world markets may be explained in terms of the endogenous fluctuations generated by the presence of nonlinearities. We then replace with a sigmoid adaptive best response mechanism, characterized by the presence of two horizontal asymptotes, the linear partial best response mechanism considered in Mamada and Perrings (2020), where the effect produced by quadratic emission charges on the dynamics of a Cournot duopoly model with homogeneous goods was investigated. Due to the sigmoid adaptive mechanism, output variation in each period depends also on current production volume. Moreover, the sigmoid nonlinearity, in addition to being well suited to describe the bounded output variations caused by physical, historical and institutional constraints, makes the model able to generate interesting, non-divergent dynamic outcomes, despite the linearity of the demand function and of marginal costs. Additionally,

*E-mail address: ahmad.naimzada@unimib.it
†E-mail address: marina.pireddu@unimib.it

following the suggestion in Mamada and Perrings (2020), we deal with the more general case of differentiated products. Beyond analytically studying the stability of the unique steady state, coinciding with the Nash equilibrium, and the effect produced by the main parameters on the stability region, we propose two dynamical approaches which allow to evaluate the environmental policy efficacy when the Nash equilibrium is not stable and thus the standard comparative statics technique does not fit for the purpose. In particular, the former approach, which is based on a comparison of emissions for different levels of charges, shows that, also in case the Nash equilibrium is not stable, the considered environmental policy may be effective both with complements and with substitutes. The latter approach, consisting in a comparison of emissions along non-stationary trajectories and along the equilibrium path, in the proposed experiments highlights that emissions are larger along non-stationary trajectories. This gives us the opportunity to show how to act on the level of the asymptotes of the sigmoid adjustment mechanism to reduce output variations, reaching at one time a complete stabilization of the system and limiting pollution.

Keywords: Cournot duopoly, emission charges, differentiated goods, sigmoid output adjustment mechanism, environmental policy efficacy, comparative dynamics.

JEL classification: C61, C62, D43, Q51, Q58

1 Introduction

According to the existing empirical literature (see e.g. Chatrath et al. 2002; Gouel 2012; Huffaker et al. 2018) the main variables, i.e., good prices and exchanged quantities, connected with real-world markets, especially those for agricultural commodities, display chaotic and erratic behaviors, including volatility. In particular, those empirical studies suggest that the therein identified dynamic phenomena may be explained in terms of the endogenous fluctuations generated by the presence of nonlinearities. Also the experimental literature (cf. for instance Arango and Moxnes 2012) concerning the real markets dynamics underlines the emergence of oscillatory behaviors in good prices and exchanged quantities. Hence, in proposing a model to describe those contexts, also in connection with ecological issues, firstly we have to guarantee that it is able to generate interesting, i.e., non-stationary, non-divergent, dynamic outcomes, so as to be "*up to the task of adequately addressing the implications of these complex system dynamics and the unpredictability which seems to be their hallmark*", quoting Stanley (2020) in regard to ecological economics. Secondly, if we are interested in investigating the effect produced by an environmental policy scheme on the generated pollution, we have to explain how the environmental policy efficacy can be evaluated in the case of non-stationary trajectories. Namely, the classical comparative statics technique, applied to the system equilibrium, which is a steady state, is not empirically grounded in such a context, in which the steady state is rarely stable. Thus, the need to develop alternative, dynamical methods arises, based for instance on the behavior of the time series of the cumulative aggregate emission. In this manner, the environmental policy efficacy, to be measured in relation to an emission reduction, could be implied by a negative variation of cumulative emissions over the considered time interval as a consequence of an increased strictness of the environmental policy scheme.

We tackle both issues by revisiting the framework in Mamada and Perrings (2020), where the effects produced by emission charges on the dynamics of a Cournot duopoly model were investigated. In more detail, motivated by the two points described above, we replace the linear partial output adjustment rule considered therein, whose linearity causes a discrepancy between the simulative outcomes and the empirical data, with a gradual sigmoid version of the best response mechanism, characterized by the presence of two horizontal asymptotes, which help avoid diverging trajectories and negativity issues. The same sigmoid formulation has been used in different macro contexts e.g. in Naimzada and Pireddu (2014, 2015), but, to the best of our knowledge, this is the first time that such nonlinearity is introduced in the decisional mechanism within a game theoretical framework. We stress that the sigmoid output adjustment rule, in addition to opening the door to complex dynamics and to giving us the opportunity to develop the above mentioned methods to test the environmental policy efficacy, is also sensible from an economic viewpoint, since it is well-suited to describe the bounded output variations caused by physical, historical and institutional constraints. Namely, when the difference between the best response and the current output level of a firm is positive, capacity constraints will bound the increase in the production volume, because of the limited expansion from time to time of capital and labor stock. When instead the difference between the best response and the current output level of a firm is negative, capital cannot

be destroyed proportionally to that difference as the only factors that may lower productivity are attrition of machines from wear, time, and obsolescence. Additionally, the labor factor imposes constraints, too: indeed, due to the presence of trade unions, it is difficult, or impossible, to reduce employment below a certain threshold level. Notice that the proposed sigmoid adjustment mechanism is suitable to describe also the gradual output variations deriving from the limits imposed by an environmental policy scheme aiming at containing pollution by bounding production, due to the direct proportionality linking them. In fact, acting on the levels of the horizontal asymptotes we obtain a further tool to contain pollution, which stabilizes the dynamics, too. The latter aspect turns out to be particularly relevant when emissions are larger along non-stationary trajectories than along equilibrium paths. In such cases, reducing output variations by lowering the distance between the asymptotes allows at one time to decrease the system dynamic complexity and to limit pollution. Moreover, with respect to the original setting in Mamada and Perrings (2020), where the goods produced by the two firms were homogeneous, we assume that firms produce differentiated goods, following the suggestion contained in the concluding section of their work. On the other hand, in regard to emission charges, we stick to the quadratic formulation considered therein.
As concerns the existing literature, we stress that in Naimzada and Pireddu (2023) we extended the setting in Mamada and Perrings (2020) by introducing differentiated goods, but without altering the output adjustment rule, while the effect played by the introduction of differentiated goods and of a nonlinear output adjustment mechanism in the framework by Mamada and Perrings (2020) has been investigated in Matsumoto et al. (2022). However, in the latter work goods can be just substitutes, not complements, and the quadratic emission charges can only be convex, without the linear term considered in Mamada and Perrings (2020), so that the environmental policy is always effective in the setting by Matsumoto et al. (2022). Furthermore, in their context the nonlinearity is represented by output dependent factors that replace the constant adjustment coefficients in the best reply mechanism by Mamada and Perrings (2020), implying that the system admits two boundary equilibria, in addition to the internal equilibrium corresponding to the one in Mamada and Perrings (2020). Moreover, Matsumoto et al. (2022) deal with the case in which marginal production costs do not coincide across firms and analyze, among other issues, the conditions for market transitions between duopoly and monopoly.

Turning back to the here considered setting, in studying it we start by analyzing the stability of the unique steady state, which coincides with the Nash equilibrium, common to the framework in Naimzada and Pireddu (2023), as well as its bifurcations and the role played by the main model parameters, finding that the equilibrium is stable when the two goods are nearly independent, while complex dynamics can arise when the dependence degree between the two goods is strong enough, despite the linearity of the demand function and of marginal costs. We recall that when the steady state is unstable in Mamada and Perrings (2020) the output quantities produced by the two firms tend instead to become unbounded, positive or negative. Furthermore, due to the introduction of the sigmoid adjustment mechanism, the equilibrium stability region is reduced in the here analyzed context with respect to Naimzada and Pireddu (2023). On the other hand, as long as the Nash equilibrium is stable in our framework, and we can thus rely on the classical comparative statics approach, we find a confirmation of the static results obtained in Naimzada and Pireddu (2023), which showed that the considered environmental policy becomes detrimental when emission charges increase too slowly with production. In order to deal with the cases in which the Nash equilibrium is not stable, we propose two alternative, dynamic approaches to evaluate the environmental policy efficacy, based either on a comparison of emissions for different levels of charges or on a comparison of emissions along non-stationary trajectories and along the equilibrium path. The proposed techniques are mainly numerical in nature, involving non-stationary orbits. The former approach shows that, also when the Nash equilibrium is not stable, the considered environmental policy may be effective in reducing pollution, both with complements and substitutes. In regard to the latter approach, since in the proposed experiments it happens that emissions are larger along non-stationary trajectories than along the equilibrium path, we explain how to act on the levels of the asymptotes of the sigmoid in view of reducing output variations, reaching a complete stabilization of the system and limiting pollution.
We stress that, to the best of our knowledge, the existing literature on ecological economics is either static (see for instance Ganguli and Raju 2012, Matsumoto and Szidarovszky 2022, Raju and Ganguli 2013, Sato 2017) or, even when the proposed models are dynamical in nature, the focus is on the behavior of the steady state (cf. e.g. Mamada and Perrings 2020, Matsumoto and Szidarovszky 2021, Matsumoto et al. 2018a, 2018b, Sarafopoulos and Papadopoulos 2017) and the investigation of the efficacy of the considered

environmental policy in non-stationary regimes is neglected. A partial exception is represented by Matsumoto et al. (2022), where the authors study the dynamic outcomes of their nonlinear model, while the environmental policy efficacy is granted by the assumptions made therein. Notice that the nonlinearities considered in the present work and in Matsumoto et al. (2022) concern the decisional mechanism, even if in a different manner, as explained in Section 2.
Indeed, the remainder of the paper is organized as follows. In Section 2 we present the setting that we consider. In Section 3 we perform the model stability analysis. In Section 4 we investigate the efficacy of the environmental policy from a dynamic viewpoint. In Section 5 we briefly discuss our results and describe possible extensions of the here studied framework.

2 The model

The extension to differentiated goods of the framework in Mamada and Perrings (2020) has been briefly presented in Naimzada and Pireddu (2023). For the reader's convenience and in order to add some important aspects in its derivation, in what follows we describe the main steps related to its static part, turning then to illustrating the sigmoid best response mechanism, which allows us to keep the same Nash equilibrium found in Naimzada and Pireddu (2023), solving at the same time the issue with diverging trajectories when equilibrium stability is lost in the linear framework. Namely, the new formulation choice allows for more realistic dynamic outcomes, suitable to mimic the volatility displayed by the variables involved in real-world markets. Moreover, from the modeling viewpoint, the sigmoid adjustment mechanism is appropriate to describe the gradual output variations caused by material, historical and institutional constraints in the production side of an economy, as well as by the limits imposed by an environmental policy scheme on production levels, due to their direct proportionality with emissions.[1]

[1]Indeed, in Section 4 we shall show that acting on the position of the sigmoid map asymptotes may represent a form of *direct* intervention on output and emission levels through a modification in the bound to the strategy variation between one period and the following one, in contrast with the *indirect* nature of the pollution control obtained by means of emission charges in (2.2). Furthermore, by changing the position of the asymptotes we will make the system converge toward the Nash equilibrium, starting from a situation characterized by the presence of a different (periodic or complex) attractor, so

Denoting by $q_{i,t+1}$ the output level of firm i at time $t+1$ and by $q^e_{j,t+1}$ the output level of firm j at time $t+1$ expected by firm i at the end of period t, with $i \neq j \in \{1,2\}$, we assume that in time period $t+1 \in \mathbb{N} \setminus \{0\}$ firm $i \in \{1,2\}$ maximizes the expected profit function

$$\pi^e_{i,t+1} = (p - \beta q_{i,t+1} - \gamma q^e_{j,t+1})q_{i,t+1} - cq^2_{i,t+1} - C_{i,t+1} \tag{2.1}$$

where p, c are positive parameters and $C_{i,t+1}$ is the emission charge, faced at time $t+1$ by firm i, that we will describe in (2.2). For the parameters β and γ, as usual in the case of differentiated goods, we suppose that $|\gamma| < \beta$.
We recall that, according to Singh and Vives (1984), the expression for the inverse demand function entering (2.1) can be derived by assuming that in an economy with a monopolistic sector with two firms, each one producing a differentiated good, and a competitive numeraire sector, there is a continuum of consumers of the same type with a utility function separable and linear in the numeraire good, so that there are no income effects on the monopolistic sector, and it is possible to perform partial equilibrium analysis. In symbols, the representative consumer has to maximize in each time period $U(q_1,q_2) - \rho_1 q_1 - \rho_2 q_2$, where ρ_i is the price of good i and $U(q_1,q_2) = p_1q_1 + p_2q_2 - \frac{1}{2}\left(\beta_1 q_1^2 + \beta_2 q_2^2 + 2\gamma q_1 q_2\right)$, with p_i and β_i positive, $\beta_1\beta_2 - \gamma^2 > 0$ and $p_i\beta_j - p_j\gamma > 0$ for $i \neq j \in \{1,2\}$. Dealing, like in Mamada and Perrings (2020), with the simplified case in which $p_1 = p_2 = p$ and $\beta_1 = \beta_2 = \beta$, the utility function reads as $U(q_1,q_2) = p(q_1+q_2) - \frac{\beta}{2}\left(q_1^2 + q_2^2\right) - \gamma q_1 q_2$, with p and β positive, and $|\gamma| < \beta$, as supposed above. In particular, if $\gamma > 0$ utility decreases when consuming the two goods together, i.e., they are substitutes; if $\gamma < 0$ utility increases when consuming the two goods together, i.e., they are complements; if $\gamma = 0$ utility is not affected by a joint consumption of the two goods, i.e., they are independent. The homogeneous good framework is obtained in the limit case $\gamma = \beta = k$, where k is the price-depressing effect of oligopoly. Taking the FOC of $U(q_1,q_2) - \rho_1 q_1 - \rho_2 q_2$, it is straightforward to obtain $\rho_i = p - \beta q_i - \gamma q_j$ for $i \neq j \in \{1,2\}$ as inverse demand functions. Further details can be found in Motta (2004) and in Singh and Vives (1984).
Concerning $C_{i,t+1}$, Mamada and Perrings (2020), followed by Naimzada and Pireddu (2023), propose the quadratic formulation for emission charges

$$C_{i,t+1} = bu_{i,t+1} + \frac{1}{2}du^2_{i,t+1}, \tag{2.2}$$

that comparative statics results become economically grounded.

with $b > 0$, $d \in \mathbb{R}$ and where, denoting by $\varepsilon > 0$ the emissions per unit output, $u_{i,t+1} = \varepsilon q_{i,t+1}$ are emissions by firm $i \in \{1, 2\}$ at time $t+1$. Mamada and Perrings (2020) use d as bifurcation parameter, finding that it has a stabilizing effect on the system equilibrium in the case of homogeneous goods. Moreover, the sign of d determines if the marginal emission charge

$$\frac{dC_{i,t+1}}{du_{i,t+1}} = b + du_{i,t+1}$$

is positive or negative. Since the marginal emission charge cannot be negative, when $d < 0$ the constraint

$$0 < q_{i,t+1} < \frac{-b}{\varepsilon d} \tag{2.3}$$

emerges. Notice that, *ceteris paribus*, an increase in d produces a raise in emission charges in (2.2) both when d is positive and when it is negative. However, in the former case the marginal emission charge increases with u, while in the latter case it decreases. In such eventuality, according to (2.3), the maximum value u can assume is given by $-b/d$. See Figure 1 for a graphical illustration.

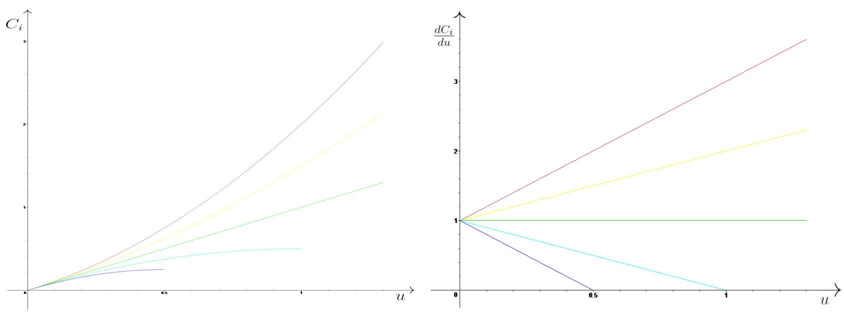

(A) (B)

Figure 1: In (A) we draw the graph of C_i in (2.2) as a function of u for $b = 1$, and $d = -2$ in blue, $d = -1$ in cyan, $d = 0$ in green, $d = 1$ in yellow, $d = 2$ in orange. In (B) we represent the corresponding marginal emission charges $\frac{dC_i}{du}$ as a function of u, using the same color distribution as in (A).

Turning back to (2.1), since

$$\frac{\partial \pi^e_{i,t+1}}{\partial q_{i,t+1}} = p - b\varepsilon - (2(\beta + c) + d\varepsilon^2)q_{i,t+1} - \gamma q^e_{j,t+1} \tag{2.4}$$

for $i \neq j \in \{1, 2\}$, expected profits are strictly concave when

$$2(\beta + c) + d\varepsilon^2 > 0. \tag{2.5}$$

This condition is satisfied when C_i in (2.2) is convex for $i \in \{1, 2\}$, i.e., for $d \geq 0$, as well as for $d \in \left(-\frac{2(\beta+c)}{\varepsilon^2}, 0\right]$, in which case C_i is concave, but production variations lead to emission charge variations close to those that we would have in the linear case, corresponding to $d = 0$. Assumption (2.5) will be maintained along the manuscript. Moreover, setting $\partial\pi^e_{i,t+1}/\partial q_{i,t+1}$ in (2.4) equal to 0 we obtain

$$R_{i,t+1}(q^e_{j,t+1}) = \frac{p - b\varepsilon - \gamma q^e_{j,t+1}}{2(\beta + c) + d\varepsilon^2} \tag{2.6}$$

as best response function for $i \neq j \in \{1, 2\}$, representing the optimal strategy for firm i in period $t + 1$, given the strategy for firm j expected by firm i for that same period. Notice that $R_{i,t+1}(q^e_{j,t+1})$ is well defined under (2.5). In order not to overburden notation, we will denote it simply by $R_i(q^e_{j,t+1})$.
Imposing like in Mamada and Perrings (2020) that firms have static expectations, it holds that $q^e_{j,t+1} = q_{j,t}$, so that (2.6) can be rewritten as

$$R_i(q^e_{j,t+1}) = R_i(q_{j,t}) = \frac{p - b\varepsilon - \gamma q_{j,t}}{2(\beta + c) + d\varepsilon^2}\,. \tag{2.7}$$

Hence, calling (q^*_1, q^*_1) the solution to the system

$$\begin{cases} q_{1,t} = R_1(q_{2,t}) \\ q_{2,t} = R_2(q_{1,t}) \end{cases}$$

in each time period t, which arises by supposing that both firms simultaneously produce the best response output to their opponent's strategy, we find like in Naimzada and Pireddu (2023) that the unique (symmetric) Nash equilibrium is given by

$$(q^*_1, q^*_2) = \left(\frac{p - b\varepsilon}{2(\beta + c) + d\varepsilon^2 + \gamma}, \frac{p - b\varepsilon}{2(\beta + c) + d\varepsilon^2 + \gamma}\right). \tag{2.8}$$

In order to avoid negativity issues, we can assume that $p > b\varepsilon$ and that $2(\beta + c) + d\varepsilon^2 + \gamma > 0$, similar to what done by Mamada and Perrings (2020) in the case of homogeneous products, or we can suppose that $p < b\varepsilon$ and $2(\beta+c)+d\varepsilon^2+\gamma < 0$. In analogy with Naimzada and Pireddu (2023), taking into account also (2.5), we will need to split the model analysis in Section 3 according to those two scenarios in the case of complements, while with substitutes the numerator and the denominator of the Nash equilibrium can just be positive.

As mentioned at the beginning of the section, we will deal with a sigmoid best response mechanism, which on the one hand allows for nontrivial and realistic erratic dynamic outcomes, and, on the other hand, is suitable to describe the gradual output variations deriving both from the limits imposed by an environmental policy scheme aiming at containing pollution by bounding production, as well as from the technical and institutional constraints that pertain the production side of an economy. Namely, when the difference between the best response and the current output level is positive, capacity constraints will bound the increase in the production volume, due to the limited expansion from time to time of capital and labor stock; when instead the difference between the best response and the current output level is negative, capital cannot be destroyed proportionally to that difference as the only factors that may reduce productivity are attrition of machines from wear, time, and obsolescence. Furthermore, also the labor factor imposes limits: indeed, due to the presence of trade unions, it is difficult, or impossible, to reduce employment below a certain threshold level. In more detail, firms, due to an adjustment capacity constraint, in Mamada and Perrings (2020) and in Naimzada and Pireddu (2023) modify their output level according to the size and the extent of the difference between the best response and the current output level in just a partial way. However, rather than the linear formulation adopted in Mamada and Perrings (2020) and in Naimzada and Pireddu (2023)

$$q_{i,t+1} = q_{i,t} + \lambda(R_i(q_{j,t}) - q_{i,t}), \tag{2.9}$$

where, for $i \neq j \in \{1,2\}$, $R_i(q_{j,t})$ is the best response function of firm i at time $t+1$ to the output $q_{j,t}$ produced by firm j at time t and the reactivity parameter λ varies in $(0,1)$, we will now consider

$$q_{i,t+1} = q_{i,t} + \delta\left(\frac{\upsilon+\delta}{\upsilon\, e^{-\sigma(R_i(q_{j,t})-q_{i,t})}+\delta} - 1\right), \tag{2.10}$$

where $R_i(q_{j,t})$ is still the best response function in (2.7).
Moving $q_{i,t}$ to the left-hand side of (2.10), we obtain that the output variation

of firm $i \neq j \in \{1, 2\}$ between the next period and the current one is described by the sigmoid map

$$g(x) := \delta \left(\frac{\upsilon + \delta}{\upsilon \, e^{-\sigma x} + \delta} - 1 \right), \tag{2.11}$$

with x measuring the difference between the next period optimal strategy and the current output volume, so that (2.10) can be rewritten as

$$q_{i,t+1} - q_{i,t} = g(R_i(q_{j,t}) - q_{i,t}). \tag{2.12}$$

Before looking at the features of g, let us introduce the concept of *relative variation*, that we will denote by $\mathcal{RV}$, and which at time t for firm i is defined as

$$\mathcal{RV}_{i,t} := \frac{q_{i,t+1} - q_{i,t}}{R_i(q_{j,t}) - q_{i,t}}, \tag{2.13}$$

with $i \neq j \in \{1, 2\}$, i.e., as the ratio between the output variation in a given period and the difference between the optimal output and the current strategy. Thanks to such notion, we will be able to compare in a more formal manner our adjustment mechanism in (2.10) with that in (2.9), considered by Mamada and Perrings (2020), as well as with the nonlinear updating rule adopted by Matsumoto et al. (2022), which reads as

$$q_{i,t+1} = q_{i,t} + K q_{i,t}(R_i(q_{j,t}) - q_{i,t}), \tag{2.14}$$

for $i \neq j \in \{1, 2\}$ and $K \in (0, +\infty)$.
Computing the relative variation in the three different scenarios, we obtain $\mathcal{RV}_{i,t} = \lambda$ in relation to (2.9), $\mathcal{RV}_{i,t} = K q_{i,t}$ in relation to (2.14), while $\mathcal{RV}_{i,t}$ has no explicit formulation in connection with (2.10), but we will derive below some qualitative properties for it. The common feature for the relative variation in the three settings is that it is always linked with the reactivity, given just by λ for (2.9), by K for (2.14), and by σ for (2.10). Of course, the connection between the relative variation and the reactivity is different in each case. Indeed, in Mamada and Perrings (2020) the two notions coincide, the relative variation being constant, while in the setting by Matsumoto et al. (2022), that may be considered as an extension of the former framework, the relative variation proportionally increases with the current production volume, the proportionality factor being given by the reactivity. Also in regard to the sigmoid adjustment rule in (2.10), the relative variation is not

constant, depending on the current production level.
Turning back to the mechanism in (2.12), we notice that g in (2.11) is increasing and that it passes through the origin. Moreover, it is bounded from below by $-\delta$ and from above by υ. The presence of the two horizontal asymptotes helps avoid diverging trajectories and negativity issues. In particular, by raising (resp. lowering) υ and δ we obtain an increase (resp. decrease) in the possible output variations, which have to be contained in the interval $(-\delta, \upsilon)$. Notice that acting on υ (resp. δ) produces an effect when the best response is above (resp. below) the current production level. We show the graph of the sigmoid function g for different values of the reactivity σ in Figure 2, where we denote by y the output difference between tomorrow and today output levels by firm i. Namely, σ is a non-negative parameter describing the intensity with which the difference between the best response and the current output level determines the output variation. For $\sigma = 0$, firms are completely insensitive to that difference and they keep their output unchanged in time, so that $q_{i,t+1} - q_{i,t} = 0$ for every t. In the limit $\sigma \to +\infty$, the sigmoid approaches a piecewise constant function, taking just the lowest and the highest possible values: indeed, the value of g coincides with $-\delta$ for negative values of the signal $R_i(q_{j,t}) - q_{i,t}$ and with υ for positive values of $R_i(q_{j,t}) - q_{i,t}$. Moreover, as observed above, σ influences, together with υ and δ, the relative variation in connection with (2.12), that, recalling (2.13), is given by

$$\mathcal{RV}_{i,t} = \frac{g(R_i(q_{j,t}) - q_{i,t})}{R_i(q_{j,t}) - q_{i,t}}. \tag{2.15}$$

Notice that, looking at (2.10) and recalling the meaning of variable x introduced after (2.11), $x = 0$ corresponds to the Nash equilibrium (q_1^*, q_2^*) in (2.8), as the best response function formulation is still the one in (2.7). Since g is an increasing map passing through the origin, $x = 0$ coincides also with the unique steady state for (2.10). Some features of $\mathcal{RV}_{i,t}$ easily follow from (2.11) and (2.15), observing that: (I) $g(x)/x \to 0^+$ when $x \to \pm\infty$;
(II) $g(x)/x$ is an even map when $\upsilon = \delta$;

$$\text{(III)} \qquad \frac{g(x)}{x} \to \widetilde{\sigma} := \frac{\upsilon\delta\sigma}{\upsilon + \delta} \quad \text{when} \quad x \to 0. \tag{2.16}$$

Namely, (I) implies that for us there is no direct proportionality between $\mathcal{RV}_{i,t}$ and $q_{i,t}$, contrary to what occurs in the setting by Matsumoto et al. (2022), where with (2.14) the relative variation proportionally increases with the current production volume. Indeed, with (2.10) $\mathcal{RV}_{i,t}$ tends to vanish when the production volume is far from the current optimal output level. In particular, due to (II), such decrease in $\mathcal{RV}_{i,t}$ is symmetric with respect to positive or negative values of the signal $R_i(q_{j,t}) - q_{i,t}$ that have the same modulus if the upper and lower asymptotes of g are at the same distance from the horizontal axis. Finally, by (III) in (2.16) the relative variation at the steady state coincides with $\widetilde{\sigma}$, which, taking into account the joint effect of σ, υ and δ, will be called joint reactivity in what follows. Notice that σ influences $\widetilde{\sigma}$, without modifying the value of the asymptotes and that, like in the linear framework proposed by Mamada and Perrings (2020) it would be possible to consider different values of the reactivity parameter λ for the two firms, also in the present nonlinear setting we could assume personalized values of the sensitivity parameter σ. However, since this hypothesis would overburden the analysis, making the interpretation of the results less neat, similar to Mamada and Perrings (2020), where the reactivity parameter is homogeneous for the two firms, we prefer to deal with the case in which the value of σ coincides for firms.

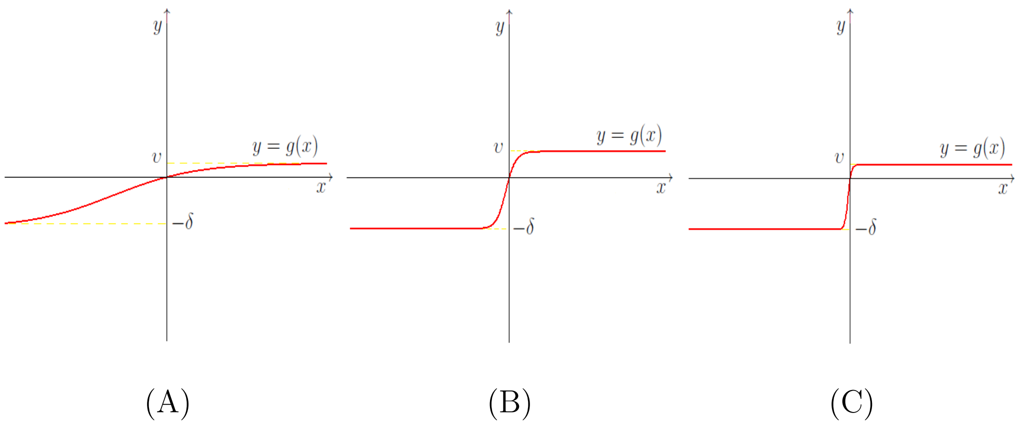

Figure 2: The graph of the sigmoid function g in (2.11), for a low (in (A)), intermediate (in (B)) and high (in (C)) value of σ.

3 Local stability analysis

Let us start by investigating how the presence of the sigmoid adjustment mechanism influences, with respect to the linear framework with differentiated goods considered in Naimzada and Pireddu (2023), the local stability of the Nash equilibrium for (2.10), which for $i \neq j \in \{1, 2\}$ may be explicitly written as

$$\begin{cases} q_{1,t+1} = q_{1,t} + \delta \left(\frac{\upsilon+\delta}{\upsilon\, e^{-\sigma\left(R_1(q_{2,t})-q_{1,t}\right)}+\delta} - 1 \right) = q_{1,t} + \delta \left(\frac{\upsilon+\delta}{\upsilon\, e^{-\sigma\left(\frac{p-b\varepsilon-\gamma q_{2,t}}{2(\beta+c)+d\varepsilon^2}-q_{1,t}\right)}+\delta} - 1 \right) \\ q_{2,t+1} = q_{2,t} + \delta \left(\frac{\upsilon+\delta}{\upsilon\, e^{-\sigma\left(R_2(q_{1,t})-q_{2,t}\right)}+\delta} - 1 \right) = q_{2,t} + \delta \left(\frac{\upsilon+\delta}{\upsilon\, e^{-\sigma\left(\frac{p-b\varepsilon-\gamma q_{1,t}}{2(\beta+c)+d\varepsilon^2}-q_{2,t}\right)}+\delta} - 1 \right) \end{cases} \tag{3.1}$$

Calling $F : (0, +\infty)^2 \to (0, +\infty)^2$ the planar map associated with the above dynamical system, in Subsection 3.1 we will deal with the cases of substitutable and independent goods, in which $\gamma \in [0, \beta)$, so that the framework with homogeneous goods, corresponding to $\gamma = \beta$, is encompassed as limit case, while in Subsection 3.2 we will focus on complements, with $\gamma \in (-\beta, 0)$.

3.1 Substitutable and independent goods

In the present subsection, we deal with the case $\gamma \in [0, \beta)$. Since (2.5) has to be satisfied, it follows that $2(\beta + c) + d\varepsilon^2 + \gamma > 0$. Hence, the positivity of the Nash equilibrium (q_1^*, q_2^*) in (2.8) requires that

$$p - b\varepsilon > 0, \tag{3.2}$$

similar to Mamada and Perrings (2020). Consequently, the following result, which highlights the destabilizing role of the joint reactivity $\widetilde{\sigma} = \frac{\upsilon\delta\sigma}{\upsilon+\delta}$ introduced in (2.16), holds true:

Proposition 3.1 *When* $\gamma \geq 0$*, under* (2.5) *and* (3.2)*,* (q_1^*, q_2^*) *in* (2.8) *is admissible according to* (2.3) *for* $d > -\frac{b(2\beta+2c+\gamma)}{\varepsilon p}$*. If this is the case,* (q_1^*, q_2^*) *is locally asymptotically stable for System* (3.1) *when* $d > -\frac{2\beta+2c-\gamma}{\varepsilon^2}$ *and* $\widetilde{\sigma} < \frac{2}{1+\frac{\gamma}{2(\beta+c)+d\varepsilon^2}}$.

Proof. We are going to derive the local stability conditions for our system at the steady state by using Jury (1964) conditions

$$\begin{aligned} &(i) \quad \det(J) < 1; \\ &(ii) \quad 1 + \operatorname{tr}(J) + \det(J) > 0; \\ &(iii) \quad 1 - \operatorname{tr}(J) + \det(J) > 0, \end{aligned} \tag{3.3}$$

where $J = J_F(q_1^*, q_2^*)$ is the Jacobian matrix for F computed at (q_1^*, q_2^*), which reads as

$$J_F(q_1^*, q_2^*) = \begin{bmatrix} 1-\widetilde{\sigma} & -\frac{\widetilde{\sigma}\gamma}{2(\beta+c)+d\varepsilon^2} \\ -\frac{\widetilde{\sigma}\gamma}{2(\beta+c)+d\varepsilon^2} & 1-\widetilde{\sigma} \end{bmatrix} \tag{3.4}$$

and that is well defined by (2.5). Since as expressions for the determinant and for the trace of J we respectively find

$$\det(J) = \widetilde{\sigma}^2 \left(1 - \frac{\gamma^2}{(2(\beta+c)+d\varepsilon^2)^2}\right) - 2\widetilde{\sigma} + 1, \qquad \mathrm{tr}(J) = 2 - 2\widetilde{\sigma},$$

condition (iii) reads as

$$1 - \frac{\gamma^2}{(2(\beta+c)+d\varepsilon^2)^2} > 0, \tag{3.5}$$

so that, setting $A := 1 - (\gamma^2/(2(\beta+c)+d\varepsilon^2)^2)$, we have that A has to lie in the interval $(0,1)$. Condition (i) is then equivalent to

$$\widetilde{\sigma} < \frac{2}{A}, \tag{3.6}$$

while condition (ii) holds if and only if

$$A\widetilde{\sigma}^2 - 4\widetilde{\sigma} + 4 > 0. \tag{3.7}$$

It is straightforward to check that (3.6) and (3.7) are jointly satisfied when

$$\widetilde{\sigma} < \frac{2}{1 + \frac{\gamma}{2(\beta+c)+d\varepsilon^2}}. \tag{3.8}$$

Moreover, since (3.5) can be equivalently rewritten as

$$(2(\beta+c)+d\varepsilon^2-\gamma)(2(\beta+c)+d\varepsilon^2+\gamma) > 0 \tag{3.9}$$

and by (2.5) it holds that $2(\beta+c)+d\varepsilon^2+\gamma > 0$, then (3.5) is equivalent to

$$2(\beta+c)+d\varepsilon^2-\gamma > 0 \tag{3.10}$$

as well, which can be rewritten as

$$d > -\frac{2\beta+2c-\gamma}{\varepsilon^2}. \tag{3.11}$$

Since, by (2.5), the conditions in (2.3) lead to

$$d > -\frac{b(2\beta + 2c + \gamma)}{\varepsilon p}, \tag{3.12}$$

the desired conclusion follows from (3.8), (3.11) and (3.12). □

Comparing the above result with the findings obtained in Naimzada and Pireddu (2023), Proposition 3.1 highlights an overall reduction in the stability region for (q_1^*, q_2^*) with respect to Proposition 3 therein due to the introduction of the sigmoid adjustment mechanism in (2.10). Namely, under (3.2) in the nonlinear context we observe stricter conditions for stability than in its linear counterpart, arising from the destabilizing role played by the joint reactivity $\widetilde{\sigma}$ (cf. (3.8)). Specifically, when (3.8) is violated, a period-doubling bifurcation occurs at the steady state,[2] possibly opening the door to interesting dynamic phenomena. We illustrate two different scenarios, according to the sign of d, in Figure 3, where we let σ vary. More precisely, for a positive value of d, if (3.2) holds true, the only condition in Proposition 3.1 that can be violated is the last one, i.e., that in (3.8). Indeed, for the parameter configuration considered in Figure 3 (A), where $d = 0.1$, (3.8) reads as $\widetilde{\sigma} < 1.413$ or, equivalently, as $\sigma < 4.175$, since $\delta = 0.4$ and $\upsilon = 2.2$. In fact, in that bifurcation diagram σ varies in $(0, 6.5)$ and (q_1^*, q_2^*) in (2.8) is stable for low values of σ, while above the stability threshold we observe a cascade of period-doubling bifurcations leading to chaos. On the other hand, when dealing with negative values for d, no condition in Proposition 3.1 is granted. In particular, in Figure 3 (B) we fix $d = -0.4$ and, for the chosen parameter set, conditions (2.5) and (3.2) are fulfilled, as well as the stability condition in (3.11), which reads as $d > -0.480$, while (3.8) reads as $\widetilde{\sigma} < 1.089$, or equivalently $\sigma < 3.218$. Hence, like in (A), also in this case the steady state is stable for low values of σ. On the other hand, since the

[2] According to Elaydi (2007), page 249, this is a consequence of the fact that a violation of (3.8) occurs when condition *(ii)* in (3.3) becomes an equality, so that the Jacobian matrix in (3.4) admits a real eigenvalue equal to -1. Analogously, a period-doubling bifurcation occurs at the steady state with complements when (3.17) in the proof of Proposition 3.2 is violated. Of course, the same is still true when (3.8) and (3.17) are rewritten in order to make explicit a parameter different from $\widetilde{\sigma}$, such as d or γ. In this respect, we remark that a period-doubling bifurcation occurs on *increasing* $\widetilde{\sigma}$ or $|\gamma|$ (cf. Corollaries 3.5 and 3.6 for γ), while a period-doubling bifurcation occurs on *decreasing* d (see Corollaries 3.1 and 3.3). We can then equivalently say that a period-halving bifurcation occurs on increasing d.

admissibility condition in (2.3) leads to[3] $q_i < 0.370$ for $i \in \{1, 2\}$, it is fulfilled just for $\sigma \in (0, 3.660)$. This is indeed the interval for σ depicted in Figure 3 (B), where we have to interrupt the bifurcation diagram before the cascade of period-doubling bifurcations (cf. also Footnote 2). We stress that, both in (A) and in (B), orbits do not diverge when the steady state is not stable, thanks to the introduction of the sigmoid adjustment mechanism, differently from what happens with the linear adjustment rule considered in Mamada and Perrings (2020) and in Naimzada and Pireddu (2023). Notice that for the parameter configurations in Figure 3 (A) and (B), disregarding the parameters not encompassed in the model linear formulation, (q_1^*, q_2^*) in (2.8) is stable for the dynamical system analyzed in Naimzada and Pireddu (2023) since the stability condition in (3.11), common to that framework (cf. Proposition 3 therein), is fulfilled. We also stress that considering $\gamma = \beta = 3.1$ in Figure 3 (A) and (B), so that goods are homogeneous, we obtain dynamics analogous to the ones detected in those bifurcation diagrams, where the interdependence degree between goods is already very high. In particular, for the parameter configurations in Figure 3 (A) and (B) except for $\gamma = \beta = 3.1$, (q_1^*, q_2^*) in (2.8), which in the case of homogeneous goods reads as

$$(q_1^*, q_2^*) = \left(\frac{p - b\varepsilon}{3\beta + 2c + d\varepsilon^2}, \frac{p - b\varepsilon}{3\beta + 2c + d\varepsilon^2} \right),$$

is stable for the dynamical system considered in Mamada and Perrings (2020) since the stability condition in (3.11), which becomes $d > -\frac{\beta + 2c}{\varepsilon^2}$, is fulfilled for those parameter values.

In regard to comparative statics, we remark that the same conclusions contained in Propositions 1 and 2 in Naimzada and Pireddu (2023), showing that, with substitutable and independent goods, under (3.2), the components of the Nash equilibrium in (2.8) decrease when b, d or ε increase in the model linear formulation, hold true with the sigmoidal adjustment mechanism, too. Hence, the efficacy of the environmental policy described by the emission charges in (2.2) would seem not to be affected by the nonlinear output adjustment rule introduced in the present work. On the other hand, as underlined in Naimzada and Pireddu (2023), a comparative statics result is economically grounded if it concerns an equilibrium which is asymptotically stable and thus orbits converge towards it after a transient period. Due to

[3] Notice that, when the Nash equilibrium is unstable, (2.3) has to be satisfied by all production levels, not just by those computed at the equilibrium.

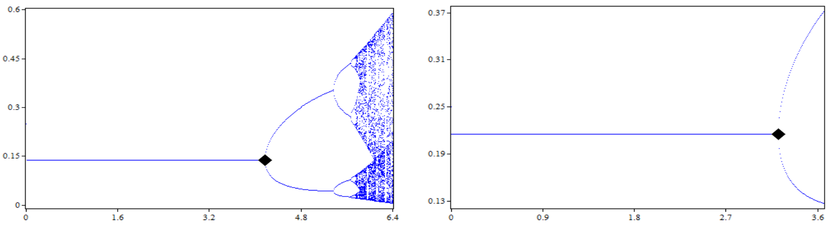

(A) (B)

Figure 3: The bifurcation diagram of $q_{1,t+1}$ in (3.1) with respect to σ and initial conditions $q_{1,0} = 0.25$, $q_{2,0} = 0.2$, for $p = 2.5$, $\delta = 0.4$, $\upsilon = 2.2$, $\beta = 3.1$, $c = 0.15$, $b = 0.4$, $\varepsilon = 2.7$, $\gamma = 3$, and $d = 0.1$ in (A), $d = -0.4$ in (B).

the above highlighted destabilizing role played by $\widetilde{\sigma}$, that concerns the case of complements, too (cf. Subsection 3.2), we can then say that the significance of the comparative statics analysis is reduced when dealing with the model nonlinear formulation in (3.1), rather than with its linear counterpart. Accordingly, in Section 4 we will present alternative, dynamic approaches to evaluate the environmental policy efficacy, based either on a comparison of emissions along non-stationary trajectories and along the equilibrium path or on a comparison of emissions for different levels of charges in (2.2), described by increasing values of d.
Still in regard to d, we observe that it is possible to rewrite the statement of Proposition 3.1 in order to make its role explicit starting from (3.8) as follows:

Corollary 3.1 *When* $\gamma \geq 0$, *under* (2.5) *and* (3.2), (q_1^*, q_2^*) *in* (2.8) *is admissible according to* (2.3) *for* $d > -\frac{b(2\beta+2c+\gamma)}{\varepsilon p}$. *If this is the case,* (q_1^*, q_2^*) *is locally asymptotically stable for System* (3.1) *for* $\widetilde{\sigma} < 2$ *and*

$$d > \max\left\{\frac{-2(\beta+c)}{\varepsilon^2} + \frac{\gamma}{\varepsilon^2}, \frac{-2(\beta+c)}{\varepsilon^2} + \frac{\gamma}{\varepsilon^2\left(\frac{2}{\widetilde{\sigma}} - 1\right)}\right\}.$$

Hence, similar to what happened with the model linear formulation in Mamada and Perrings (2020), in the case of homogeneous goods, and in Naimzada and Pireddu (2023), with substitutable and independent products, under (2.5) and (3.2) parameter d plays just a stabilizing role on the Nash equilibrium, when it influences its stability. Namely, it can also happen that, under

(2.5) and (3.2), the equilibrium in (2.8) is stable for any admissible value for d according to (2.3). However, with respect to Mamada and Perrings (2020) and Naimzada and Pireddu (2023), we now have one extra stability condition, involving $\widetilde{\sigma}$, and thus more frameworks may arise. We represent the three main possibilities[4] in Figure 4, where we take d as bifurcation parameter and the various values of p and σ allow for a different ordering among the thresholds contained in Corollary 3.1. In particular, calling d_1, d_2 the stability thresholds therein, d_0 the admissibility threshold coming from (2.3) and d_e the threshold coming from (2.5), i.e.,

$$\begin{aligned} d_1 &:= \tfrac{-2(\beta+c)}{\varepsilon^2} + \tfrac{\gamma}{\varepsilon^2}, \qquad & d_2 &:= \tfrac{-2(\beta+c)}{\varepsilon^2} + \tfrac{\gamma}{\varepsilon^2\left(\frac{2}{\widetilde{\sigma}}-1\right)}, \\ d_0 &:= -\tfrac{b(2\beta+2c+\gamma)}{\varepsilon p}, \qquad & d_e &:= -\tfrac{2(\beta+c)}{\varepsilon^2}, \end{aligned} \tag{3.13}$$

for the parameter configuration in Figure 4 (A) it holds that $d_e = -0.892 < d_2 = -0.754 < d_1 = -0.480 < d_0 = -0.469$. Since the stability thresholds d_1 and d_2 are below the admissibility threshold d_0, the Nash equilibrium is stable for all values for which it is admissible, as highlighted by the bifurcation diagram in Figure 4 (A), that we draw for $d \in (-0.469, 0)$. Moreover, the steady state is decreasing with d, in agreement with Proposition 1 in Naimzada and Pireddu (2023). On the other hand, for the parameter values considered in Figure 4 (B) it holds that $d_0 = -1.005 < d_e = -0.892 < d_2 = -0.754 < d_1 = -0.480$. Hence, although this time both stability thresholds d_1 and d_2 are larger than d_0 and satisfy (2.5), which imposes $d > d_e$, also the admissibility condition in (2.3), that leads to $q_i < -\frac{0.4}{2.7d}$ for $i \in \{1, 2\}$, since d varies, has to be taken into account. It is straightforward to check that (q_1^*, q_2^*) is admissible at the stability threshold $d = d_1$, since $q_i^* = 0.053 < -\frac{0.4}{2.7d_1} = 0.309$ for $i \in \{1, 2\}$. Hence, by continuity, it should be possible to represent the corresponding bifurcation diagram for values of d in a left neighborhood of d_1. However, due to a monotone divergence phenomenon which occurs as soon as d is below d_1, in Figure 4 (B) we draw the bifurcation diagram for $d \in [-0.480, -0.450)$ only, where the Nash equilib-

[4]Notice indeed that no crucial differences emerge when the smaller between the two stability thresholds d_1 and d_2 in (3.13) lies above or below the admissibility threshold d_0. In regard to the comparison between d_1 and d_2, with substitutes we have that $d_1 < d_2$ for $\widetilde{\sigma} > 1$. In particular, this remark applies to the limit case in which $\gamma = \beta$, i.e., when we are dealing with homogeneous goods. We finally stress that d_1 and d_2 coincide when products are independent.

rium is locally asymptotically stable.[5] We stress that at $d = d_1 = -0.480$ a saddle-node bifurcation occurs.[6] In regard to the divergence issue, we recall that the sigmoid adjustment mechanism bounds in each period the output variation and thus lowers the speed of divergence of the orbits, sometimes completely preventing divergence, like e.g. in Figures 3 and 7. However, this is not always the case, as shown by Figure 4 (B). Finally, in Figure 4 (C) we have $d_0 = -1.005 < d_e = -0.892 < d_1 = -0.480 < d_2 = -0.467$, so that also in such framework both stability thresholds d_1 and d_2 are larger than d_0 and satisfy (2.5), too. Recalling that, in the considered framework, the admissibility condition in (2.3) reads as $q_i < -\frac{0.4}{2.7d}$ for $i \in \{1, 2\}$, a simple check shows that we can represent the corresponding bifurcation diagram e.g. for $d \in (-0.478, -0.450)$. This is indeed the choice made in Figure 4 (C), which confirms that the Nash equilibrium is stable for $d > d_2$, whereas for values of d slightly smaller than d_2 we observe a cyclic behavior, since at $d = d_2$ a period-halving bifurcation occurs (cf. Footnote 2). Similar to (B), also in this case it would be possible to consider a wider range of values of d. However, since the values of q_1 raise very rapidly for decreasing values of $d \approx -0.480$, we focus on a small variation interval for d in Figure 4 (C), in order to better focus on the steady state stability recovery.

Notice that, differently from d, parameter b plays no role on the stability of the Nash equilibrium, being not present in the Jacobian matrix in (3.4).

When making explicit the effect of γ on the stability of the Nash equilibrium starting from Proposition 3.1, we obtain the following result, which shows that an increasing degree of interdependence between goods is destabilizing:

[5]Actually, it would be possible to represent the bifurcation diagram in Figure 4 (B) e.g. for $d \in [-0.480, 0)$, but, in order to better highlight what occurs in the proximity of the stability threshold $d = d_1$, we focus on a smaller interval of values for d. A similar remark applies to the choice of the range for d in the bifurcation diagram in Figure 4 (C).

[6]According to Elaydi (2007), page 249, when condition (*iii*) in (3.3) becomes an equality, and thus the Jacobian matrix in (3.4) admits a real eigenvalue equal to +1, then a fold, a pitchfork or a transcritical bifurcation occurs. Since condition (*iii*) in (3.3) becomes an equality just when (3.11) is violated, we are in one of those three cases for $d = d_1$. In particular, we can infer that a saddle-node bifurcation occurs for the parameter configuration considered in Figure 4 (B), since, according to the chosen initial conditions, the production of one firm positively diverges, while the production of the other firm negatively diverges. As we shall see in Subsection 3.2, with complements, depending on the parameter values we deal with, (*iii*) in (3.3) is either always or never fulfilled and thus no fold, pitchfork or transcritical bifurcations can occur in that framework.

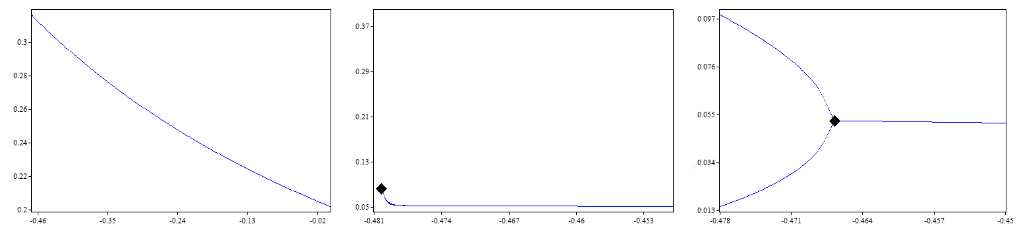

(A) (B) (C)

Figure 4: The bifurcation diagram of $q_{1,t+1}$ in (3.1) with respect to d and initial conditions $q_{1,0} = 0.25$, $q_{2,0} = 0.2$, for $\delta = 0.4$, $\upsilon = 2.2$, $\beta = 3.1$, $c = 0.15$, $b = 0.4$, $\varepsilon = 2.7$, $\gamma = 3$, and $p = 3$, $\sigma = 1.478$ in (A), $p = 1.4$, $\sigma = 1.478$ in (B), $p = 1.4$, $\sigma = 3$ in (C).

Corollary 3.2 *When* $\gamma \geq 0$, *under* (2.5) *and* (3.2), (q_1^*, q_2^*) *in* (2.8) *is admissible according to* (2.3) *for* $\gamma > -\left(2(\beta + c) + \frac{d\varepsilon p}{b}\right)$. *If this is the case, it is locally asymptotically stable for System* (3.1) *when* $\widetilde{\sigma} < 2$ *and*

$$0 \leq \gamma < \min\left\{2(\beta + c) + d\varepsilon^2, \left(\frac{2}{\widetilde{\sigma}} - 1\right)\left(2(\beta + c) + d\varepsilon^2\right)\right\}. \tag{3.14}$$

Hence, in our duopoly setting with emission charges we obtain confirmation of the destabilizing role of the degree of substitutability among commodities found by Agliari et al. (2016) in a duopoly framework with differentiated goods and nonlinear demand functions.
In regard to the threshold values in (3.14), i.e.,

$$\gamma_1 := 2(\beta + c) + d\varepsilon^2, \qquad \gamma_2 := \left(\frac{2}{\widetilde{\sigma}} - 1\right)\left(2(\beta + c) + d\varepsilon^2\right),$$

we notice that $\gamma_1 < \gamma_2$ if and only if $\widetilde{\sigma} \in (0, 1)$, while the opposite inequality holds true for $\widetilde{\sigma} \in (1, 2)$.
Rather than illustrating Corollary 3.2, we will show in Figure 7 possible bifurcation diagrams drawn for positive and negative values of γ, in relation to the findings in the more general Corollary 3.5, which encompasses both the case of substitutes and (Scenario I) of complements.

3.2 The case of complements

In the present subsection, we deal with the case $\gamma < 0$. Accordingly, under (2.5), two different scenarios ensure the positivity of the Nash equilibrium in

(2.8), i.e.,

$$p - b\varepsilon > 0, \qquad 2(\beta + c) + d\varepsilon^2 + \gamma > 0, \tag{3.15}$$

or

$$p - b\varepsilon < 0, \qquad 2(\beta + c) + d\varepsilon^2 + \gamma < 0. \tag{3.16}$$

The former scenario, in which (2.5) is granted and that occurs for small values of γ in absolute value, leads to findings similar to, but not coinciding with, those described in Subsection 3.1. In the latter scenario, that occurs for large values of γ in absolute value and for negative values of d, (2.5) is instead not guaranteed and outcomes will be drastically different from those detected in the other cases. In order to easily refer to the scenarios related to (3.15) and (3.16), in what follows we will call them Scenario I and Scenario II, respectively, and we will analyze them separately.

3.2.1 Analysis of Scenario I

The dynamic result, which represents the counterpart to Proposition 3.1, reads as follows:

Proposition 3.2 *When* $\gamma < 0$, *under* (3.15), (q_1^*, q_2^*) *in* (2.8) *is admissible according to* (2.3) *for* $d > -\frac{b(2\beta+2c+\gamma)}{\varepsilon p}$. *If this is the case, it is locally asymptotically stable for System* (3.1) *when* $\widetilde{\sigma} < \frac{2}{1-\frac{\gamma}{2(\beta+c)+d\varepsilon^2}}$.

Proof. Using Jury conditions like in the proof of Proposition 3.1, we find again (3.5), equivalent to (3.9), as well as (3.6) and (3.7). However, this time, since γ is negative, (3.6) and (3.7) are jointly fulfilled when

$$\widetilde{\sigma} < \frac{2}{1 - \frac{\gamma}{2(\beta+c)+d\varepsilon^2}}. \tag{3.17}$$

Moreover, by (3.15), (3.9) is equivalent to (3.10) and to (3.11). Since, still by (3.15), the conditions in (2.3) lead to (3.12) and it holds that

$$-\frac{b(2\beta + 2c + \gamma)}{\varepsilon p} > -\frac{2\beta + 2c + \gamma}{\varepsilon^2} > -\frac{2\beta + 2c - \gamma}{\varepsilon^2},$$

the assertion follows by (3.12) and (3.17). □

Similar to what happened with substitutes, we notice that although the same conclusions about comparative statics contained in Propositions 4 and 5 in

Naimzada and Pireddu (2023), according to which the components of the Nash equilibrium in (2.8) decrease when b, d or ε increase, hold true with the sigmoidal adjustment mechanism, too, the significance of the comparative statics analysis is reduced when dealing with the model nonlinear formulation in (3.1), since the stability region in Proposition 3.2 for (q_1^*, q_2^*) in (2.8) is reduced with respect to Proposition 6 in Naimzada and Pireddu (2023), obtained for the model linear formulation. Indeed, in that setting the Nash equilibrium is stable under (3.15) anytime it is admissible according to (2.3), i.e., when (3.12) holds true, while with the sigmoidal adjustment mechanism the extra condition in (3.17), highlighting the destabilizing role played by the joint reactivity $\widetilde{\sigma}$, is required for stability. In particular, two different possibilities, according to the sign of d, are illustrated in Figure 5, where we let σ vary, finding outcomes which bear resemblance to those detected in Figure 3, as well as some differences. Namely, for the parameter configuration considered in Figure 5 (A), where $d = 0.1$, since (3.15) holds true and (3.12) is guaranteed by the positivity of d, the only condition in Proposition 3.2 that can be violated is the one in (3.17), which reads as $\widetilde{\sigma} < 1.413$ or equivalently as $\sigma < 4.175$, since $\upsilon = 2.2$ and $\delta = 0.4$. Indeed, in that bifurcation diagram σ varies in $(0, 10)$ and (q_1^*, q_2^*) in (2.8) is stable for low values of σ, while after the period-doubling bifurcation occurring at $\sigma = 4.175$ (cf. Footnote 2), we observe a secondary Neimark-Sacker bifurcation at $\sigma = 5.112$, at which the period-two cycle loses stability and quasiperiodic dynamics emerge. When considering negative values for d, no condition in Proposition 3.2 is granted. In particular, in Figure 5 (B) we fix $d = -0.1$ and, for the chosen parameter set, condition (3.15) is fulfilled, while (3.17) reads as $\widetilde{\sigma} < 1.316$, or equivalently $\sigma < 3.888$. Hence, like in (A), also in this case the steady state is stable for low values of σ. On the other hand, since the admissibility condition in (2.3) leads to $q_i < 1.481$ for $i \in \{1, 2\}$, it is fulfilled just for $\sigma \in (0, 5.334)$. This is indeed the interval for σ depicted in Figure 5 (B), which is sufficient to witness the secondary Neimark-Sacker bifurcation of the period-two cycle, followed by quasiperiodic dynamics.[7] Both in Figure 5 (A) and (B) orbits

[7] In this respect we remark that choosing a more negative value of d would allow us to draw the bifurcation diagram for a smaller interval of values for σ. For instance, for $d = -0.15$ we should interrupt the diagram in Figure 5 (B) just after the secondary Neimark-Sacker bifurcation. The same remark applies to Figure 3. Namely, in (B) therein we have to truncate the bifurcation diagram just after the period-doubling bifurcation with $d = -0.4$, while if we chose $d = -0.1$ in Figure 3 (B), we would obtain a bifurcation diagram more similar to the one in Figure 3 (A), encompassing complex dynamics.

do not diverge after the steady state stability loss, differently from the linear framework considered in Mamada and Perrings (2020) and in Naimzada and Pireddu (2023), thanks to the introduction of the sigmoid adjustment mechanism.

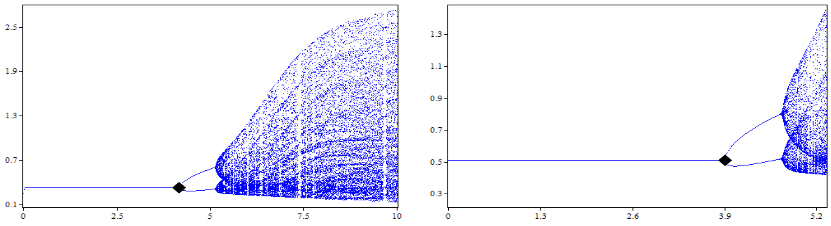

(A) (B)

Figure 5: The bifurcation diagram of $q_{1,t+1}$ in (3.1) with respect to σ and initial conditions $q_{1,0} = 0.25$, $q_{2,0} = 0.2$, for $p = 2.5$, $\delta = 0.4$, $\upsilon = 2.2$, $\beta = 3.1$, $c = 0.15$, $b = 0.4$, $\varepsilon = 2.7$, $\gamma = -3$, and $d = 0.1$ in (A), $d = -0.1$ in (B).

We stress that the threshold values in Figure 3 (A) and in Figure 5 (A) for σ coincide because in the two bifurcation diagrams we considered the same parameter values, except for $\gamma = 3$ in the former, and $\gamma = -3$ in the latter, so that $|\gamma| = 3$ in either case.[8] Namely, we will see in Corollary 3.6 in Subsection 3.3, which encompasses the frameworks of substitutes and of complements, that, since $d > 0$ in Figures 3 (A), 5 (A) and (3.2) holds true in both frameworks, then $|\gamma|$ determines the stability threshold value for $\widetilde{\sigma}$, as it follows by making the latter parameter explicit in (3.20).
Let us now state the analogues of Corollaries 3.1 and 3.2, which are obtained by highlighting in the statement of Proposition 3.2 the role of d and of γ, respectively.
In regard to the former, making d explicit in (3.17), we obtain the following:

Corollary 3.3 *When* $\gamma < 0$, *under* (3.15), (q_1^*, q_2^*) *in* (2.8) *is admissible according to* (2.3) *for* $d > -\frac{b(2\beta+2c+\gamma)}{\varepsilon p}$. *If this is the case, it is locally asymp-*

[8]Notice that in Figure 5 (B) we had to consider a different value for $d < 0$ with respect to Figure 3 (B) due to the admissibility condition (3.12), with consequent different threshold values for σ in Figures 3 (B) and 5 (B) although having $|\gamma| = 3$ in both bifurcation diagrams.

totically stable for System (3.1) *for* $\widetilde{\sigma} < 2$ *and*

$$d > \frac{-2(\beta+c)}{\varepsilon^2} - \frac{\gamma}{\varepsilon^2\left(\frac{2}{\widetilde{\sigma}}-1\right)}.$$

When illustrating the different dynamic scenarios compatible with Corollary 3.3, starting from the threshold values for d in (3.13), we notice that d_e and d_1 are no more involved, while the admissibility condition d_0 is still necessary, and, in place of d_2, we need to consider $d_2' := \frac{-2(\beta+c)}{\varepsilon^2} - \frac{\gamma}{\varepsilon^2\left(\frac{2}{\widetilde{\sigma}}-1\right)}$. Hence, the only two possibilities are given by $d_2' < d_0$ and $d_0 < d_2'$. We represent them in Figure 6 (A) and (B), respectively, where we take d as bifurcation parameter, for different values of p and σ. In more detail, with the parameter configuration in Figure 6 (A) (coinciding with that in Figure 4 (A), except for an opposite value for γ) it holds that $d_2' = -0.754 < d_0 = -0.173$. Since the stability threshold d_2' is below the admissibility threshold d_0, the Nash equilibrium is stable for all values for which it is admissible, as confirmed by the bifurcation diagram in Figure 6 (A), that we draw for $d \in (-0.173, 0)$. Notice that the steady state is decreasing with d, in agreement with Proposition 4 in Naimzada and Pireddu (2023). On the other hand, for the parameter values considered in Figure 6 (B)[9] it holds that $d_0 = -0.471 < d_2' = -0.467$. Thus, although this time the stability threshold d_2' is larger than d_0, in order to take into account the admissibility condition in (2.3), that leads to $q_i < -\frac{0.4}{2.7d}$ for $i \in \{1,2\}$, since d varies, we can represent the corresponding bifurcation diagram just for $d \in (-0.469, 0)$. However, in Figure 6 (B) we focus on $d \in (-0.469, -0.4)$, to better highlight that (q_1^*, q_2^*) is locally asymptotically stable for (3.1) when $d > d_2'$, whereas for values of d slightly smaller than d_2' we observe a cyclic behavior, that is replaced by monotone divergence for lower values of d.

Making explicit in the statement of Proposition 3.2 the role of γ rather than that of d, we obtain the next:

Corollary 3.4 *When* $\gamma < 0$, *under* (3.15), (q_1^*, q_2^*) *in* (2.8) *is admissible according to* (2.3) *for* $\gamma > -\left(2(\beta+c) + \frac{d\varepsilon p}{b}\right)$. *If this is the case, it is locally asymptotically stable for System* (3.1) *when* $\widetilde{\sigma} < 2$ *and*

$$0 > \gamma > \left(1 - \frac{2}{\widetilde{\sigma}}\right)\left(2(\beta+c) + d\varepsilon^2\right).$$

[9] We stress that with the parameter configuration in Figure 4 (B) and $\gamma = -3$ we would have found again the scenario with $d_2' < d_0$ in Figure 6 (B). Hence, in this case, unlike in (A), we had to consider a different parameter configuration with respect to Figure 4 (B).

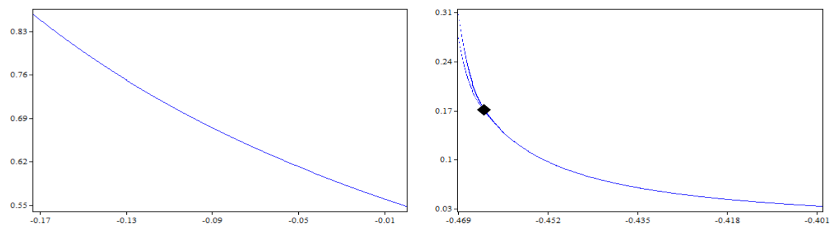

(A) (B)

Figure 6: The bifurcation diagram of $q_{1,t+1}$ in (3.1) with respect to d and initial conditions $q_{1,0} = 0.25$, $q_{2,0} = 0.2$, for $\delta = 0.4$, $\upsilon = 2.2$, $\beta = 3.1$, $c = 0.15$, $b = 0.4$, $\varepsilon = 2.7$, $\gamma = -3$, and $p = 3$, $\sigma = 1.478$ in (A), $p = 1.1$, $\sigma = 3$ in (B).

The effect on the Nash equilibrium of γ, that seems to be destabilizing in Corollary 3.2 and stabilizing in Corollary 3.4, will be better highlighted in Corollary 3.5 in Subsection 3.3, in which γ can take both positive and negative values.
Before stating that result, we complete the investigation of what occurs with complements by focusing on Scenario II.

3.2.2 Analysis of Scenario II

Even under (3.16), the conclusions about comparative statics found in Naimzada and Pireddu (2023) (cf. Propositions 7 and 8 therein) still hold true with the model nonlinear formulation, showing that the environmental policy described by the emission charges C_i in (2.2) is not effective in reducing pollution when d is negative enough and thus emission charges increase too slowly with production. Namely, under (3.16), which can be fulfilled just by values of d that are much lower than 0, the components of the Nash equilibrium in (2.8) increase with b, d and ε.
In this scenario however we find confirmation of the dynamic result in Naimzada and Pireddu (2023) (cf. Proposition 9 therein), too, according to which the steady state is never stable, when it is admissible. Namely, the counterpart to Propositions 3.1 and 3.2 reads as follows:

Proposition 3.3 *When* $\gamma < 0$, *under* (2.5) *and* (3.16), (q_1^*, q_2^*) *in* (2.8) *is admissible according to* (2.3) *for* $d < -\frac{b(2\beta+2c+\gamma)}{\varepsilon p}$. *If this is the case, it is always unstable for System* (3.1).

Proof. Using Jury conditions, we find again (3.5), equivalent to (3.9), as well as (3.6) and (3.7). However, since we are now supposing that $2(\beta+c)+d\varepsilon^2+\gamma<0$, this time from (3.9) it follows that

$$2(\beta+c)+d\varepsilon^2-\gamma<0, \tag{3.18}$$

which contradicts (2.5) with $\gamma<0$. Hence, Jury conditions are never satisfied for System (3.1) at (q_1^*, q_2^*), leading to the assertion. □

We will not illustrate the dynamics arising on increasing the main model parameters in this scenario, in which no stability thresholds are present, since the numerical simulations we performed provided divergent outcomes, with no emerging attractors.
In order to conclude the local stability analysis, we shall better highlight the role of γ. This will be done in the next subsection, where we will derive results that encompass both the case of substitutes and of complements under (3.15).

3.3 The role of the interdependence degree between goods

Merging Corollaries 3.2 and 3.4, we find the following:

Corollary 3.5 *Under* (2.5) *and* (3.15), (q_1^*, q_2^*) *in* (2.8) *is admissible according to* (2.3) *for* $\gamma > -\left(2(\beta+c)+\frac{d\varepsilon p}{b}\right)$. *If this is the case, it is locally asymptotically stable for System* (3.1) *when* $\widetilde{\sigma}<2$ *and*

$$\left(1-\frac{2}{\widetilde{\sigma}}\right)\left(2(\beta+c)+d\varepsilon^2\right)<\gamma<\min\left\{2(\beta+c)+d\varepsilon^2, \left(\frac{2}{\widetilde{\sigma}}-1\right)\left(2(\beta+c)+d\varepsilon^2\right)\right\}. \tag{3.19}$$

Although containing heavy conditions, Corollary 3.5 shows that increasing the absolute value of γ has a destabilizing effect on System (3.1).
The statement of Corollary 3.5 is much simplified under the assumption that $d>0$, in which case there is no need for the admissibility condition in (2.3), and (2.5) and (3.15) reduce to (3.2). Moreover, the stability condition (3.10) derived in Proposition 3.1 is granted, and thus we easily obtain the next:

Corollary 3.6 *Assuming that* $d>0$, *under* (3.2) *it holds that* (q_1^*, q_2^*) *in* (2.8) *is locally asymptotically stable for System* (3.1)

- *for every value of* $|\gamma| < \beta$ *if* $\widetilde{\sigma} \leq \eta := \frac{4\beta+4c+2d\varepsilon^2}{3\beta+2c+d\varepsilon^2}$;
- *for every value of* $|\gamma| < \left(\frac{2}{\widetilde{\sigma}} - 1\right)\left(2(\beta + c) + d\varepsilon^2\right)$ *if* $\eta < \widetilde{\sigma} < 2$;
- *for no values of* γ *if* $\widetilde{\sigma} \geq 2$.

Proof. For $d > 0$, (3.19) reads as

$$|\gamma| < \left(\frac{2}{\widetilde{\sigma}} - 1\right)\left(2(\beta + c) + d\varepsilon^2\right), \tag{3.20}$$

which can be fulfilled by some values of γ just when $\widetilde{\sigma} < 2$, since $2(\beta + c) + d\varepsilon^2 > 0$. Recalling that $\gamma \in (-\beta, \beta)$, (3.20) imposes stricter bounds on γ exclusively when $\left(\frac{2}{\widetilde{\sigma}} - 1\right)\left(2(\beta + c) + d\varepsilon^2\right) < \beta$, i.e., when $\widetilde{\sigma} > \eta := \frac{4\beta+4c+2d\varepsilon^2}{3\beta+2c+d\varepsilon^2} \in (1, 2)$. The proof is complete. □

We illustrate the three scenarios described in Corollary 3.6 in Figure 7, where we show the bifurcation diagram of $q_{1,t+1}$ in (3.1) for $\gamma \in (-\beta, \beta)$ and different, increasing, values of σ. Namely, for the parameter configuration considered in Figure 7 it holds that $d > 0$ and $p > b\varepsilon$, so that (3.2) is fulfilled and it is immediate to check that, in analogy with the results about comparative statics contained in the above recalled Propositions 1, 2, 4 and 5 in Naimzada and Pireddu (2023), where the role of b, d and ε was investigated, (q_1^*, q_2^*) in (2.8) is decreasing for $\gamma \in (-\beta, \beta) = (-3.1, 3.1)$. Moreover, for the parameter η introduced in Corollary 3.6 it holds that $\eta = 1.400$, and thus in Figure 7 (A), for $\sigma = 2$, we have $\widetilde{\sigma} = 0.677 < \eta$, so that the Nash equilibrium is locally asymptotically stable for every value of $\gamma \in (-3.1, 3.1)$; in Figure 7 (B), for $\sigma = 5.8$, we have $\eta < \widetilde{\sigma} = 1.963 < 2$, so that the Nash equilibrium is locally asymptotically stable just for $\gamma \in (-0.137, 0.137)$, according to (3.20); in Figure 7 (C), for $\sigma = 6$, we have $\widetilde{\sigma} = 2.030 > 2$, so that the Nash equilibrium is stable for no values of γ. We finally observe that, as highlighted by Figure 7 (B) and (C), when the steady state loses stability, via period-doubling bifurcations (cf. Footnote 2), because of an high interdependence degree between goods, complex dynamics may emerge due to the presence of chaotic or quasiperiodic attractors, but no divergence issues arise thanks to the bounds imposed by the sigmoidal function in (3.1).

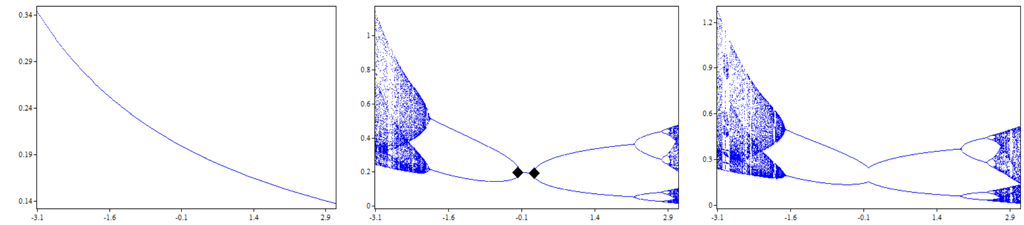

(A) (B) (C)

Figure 7: The bifurcation diagram of $q_{1,t+1}$ in (3.1) for $\gamma \in (-3.1, 3.1)$ and initial conditions $q_{1,0} = 0.25$, $q_{2,0} = 0.2$, for $p = 2.5$, $\delta = 0.4$, $\upsilon = 2.2$, $\beta = 3.1$, $c = 0.15$, $b = 0.4$, $d = 0.1$, $\varepsilon = 2.7$, and $\sigma = 2$ in (A), $\sigma = 5.8$ in (B), $\sigma = 6$ in (C).

4 Dynamic approaches for the evaluation of the environmental policy efficacy

We now discuss how to evaluate the environmental policy efficacy when the steady state is not stable. Namely, in introducing our model we stressed that a growing empirical literature (see e.g. Chatrath et al. 2002; Gouel 2012; Huffaker et al. 2018) highlights the chaotic behavior of the main variables in various markets, and in particular in agricultural markets. In order to be realistic, our model has to be able to reproduce the dynamic phenomena identified by those empirical studies, according to which what we see is the result of the action of underlying nonlinear mechanisms. Starting then from the framework in Mamada and Perrings (2020), we replaced the linear output adjustment rule considered therein with a sigmoid mechanism in view of obtaining interesting, i.e., non-stationary, non-divergent, dynamic outcomes. The introduction of the sigmoid mechanism, in addition to allowing for nontrivial dynamics, shrinks the steady state stability region. Indeed, comparing Propositions 3.1, 3.2 and 3.3 with the corresponding results in Naimzada and Pireddu (2023), we observe a reduction in the stability region for (q_1^*, q_2^*) both in the case of substitutes and of complements in Scenario I - in the latter framework the Nash equilibrium in Naimzada and Pireddu (2023) was always stable when admissible - and a confirmation of its unconditional instability in Scenario II, in consequence of the introduction of the sigmoid adjustment mechanism in (2.10). Therefore, it is important to understand how the environmental policy efficacy can be evaluated in the case of non-stationary trajectories. Namely, as long as the Nash equilibrium is stable, such as in Figures 4 (A) and 6 (A), the efficacy of the environmental policy can be assessed using the standard tool, which is represented by the comparative statics analysis. In this respect, we recall that, as mentioned in Section 3, according to Propositions 1 and 4 in Naimzada and Pireddu (2023), which hold true with the nonlinear adjustment mechanism in (2.10), too, the environmental policy described by the emission charges C_i in (2.2) is effective in reducing pollution, i.e., the equilibrium pollution level falls with an increase in b or d, with substitutes or under (3.15), while in agreement with Proposition 7 in Naimzada and Pireddu (2023) it is detrimental under (3.16), since in such case the equilibrium pollution level raises with an increase in b or d, due to the fact that, under (3.16), emission charges increase too slowly with production. Nonetheless, when the steady state is not stable, or when the considered scenario is characterized by the presence of an attractor different from the Nash equilibrium, the comparative statics technique is neither economically, nor empirically grounded. In such cases, we then need to introduce alternative methods, based for instance on the behavior, for different values of d, of the time series of the cumulative emissions, defined as the sum, over a certain time interval $[0, T]$, of the aggregate emissions $U_t := u_{1,t} + u_{2,t} = \varepsilon(q_{1,t} + q_{2,t})$ produced in time period $t \in [0, T]$ by both firms, i.e., in symbols $CE_T := \sum_{t=0}^{T} U_t = \varepsilon \sum_{t=0}^{T}(q_{1,t} + q_{2,t})$. In this manner, the environmental policy efficacy could be implied by a negative variation of cumulative emissions over the chosen time interval as a consequence of an increase in d. We can use such method to investigate the environmental policy efficacy e.g. in the contexts considered in Figures 4 (C) and 6 (B), where d was the bifurcation parameter.

To that aim, for the parameter values used therein we reproduce the two bifurcation diagrams for aggregate emissions U_{t+1} in Figure 8 (A) and (C), respectively, where we fix three different values of d (colored in blue, red and green), some of which lie in the interval where the steady state is unstable, while the remaining ones belong to the stability interval of the Nash equilibrium. We show the corresponding time series of the cumulative emissions CE_T for $T \in [0, 100]$ in Figure 8 (B) and (D), by using the same colors as in (A) and (C). In particular, in Figure 8 (A) and (B) the blue color refers to $d = -0.477$, the red color to $d = -0.471$ and the green color to $d = -0.465$, while in Figure 8 (C) and (D) the blue color refers to $d = -0.468$, the red

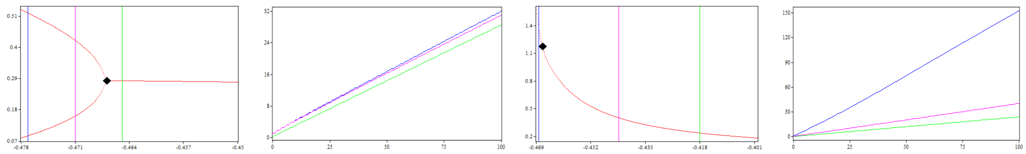

(A) (B) (C) (D)

Figure 8: In (A) and (C) we report the bifurcation diagrams of U_{t+1} with respect to d for the same parameter values used in Figures 4 (C) and 6 (B), respectively. In (B) and (D) we show the time series of cumulative emissions CE_T for $T \in [0, 100]$ corresponding to the values of d marked with different colors in (A) and (C), respectively. The initial conditions in (B) are $U_0 = \varepsilon(q_{1,0} + q_{2,0}) = 2.7 * 0.45 = 1.215$, connected with $q_{1,0} = 0.25$ and $q_{2,0} = 0.2$, for the blue and the red time series, and $2\varepsilon q_1^* = 2 * 2.7 * 0.052 = 0.281$ for the green time series, while in (D) the initial conditions are $U_0 = 2.7 * 0.45 = 1.215$, connected with $q_{1,0} = 0.25$ and $q_{2,0} = 0.2$, for the blue time series, $2\varepsilon q_1^* = 2 * 2.7 * 0.074 = 0.399$ for the red time series, and $2\varepsilon q_1^* = 2 * 2.7 * 0.044 = 0.238$ for the green time series.

color to $d = -0.443$ and the green color to $d = -0.418$. The initial conditions in (B) are $U_0 = \varepsilon(q_{1,0} + q_{2,0}) = 2.7 * 0.45 = 1.215$ for the blue and the red time series, and $2\varepsilon q_1^* = 2 * 2.7 * 0.052 = 0.281$ for the green time series, while in (D) the initial conditions are $U_0 = 2.7 * 0.45 = 1.215$ for the blue time series, $2\varepsilon q_1^* = 2 * 2.7 * 0.074 = 0.399$ for the red time series, and $2\varepsilon q_1^* = 2 * 2.7 * 0.044 = 0.238$ for the green time series. Since in (B) and (D) the cumulative emissions for $T \in [0, 100]$ are larger for lower values of d, this means that increasing emission charges in (2.2) reduce pollution, and thus the considered environmental policy is effective. We would find the same conclusion by applying the just described method to the framework in Figure 4 (B), too, in agreement with the comparative statics result for Figure 4 (A) (see Proposition 1 in Naimzada and Pireddu, 2023). Contrasting Figure 8 (B) and (D), we observe that, although in both (A) and (C) the considered values of d are equidistant, pollution decreases in (B) rapidly for higher values of d, while in (D) the efficacy of the environmental policy, although raising with d, slows down when d increases. In this sense, an intense increase in d is more useful in (B) than in (D).
In view of better comparing and understanding Figure 8 (A) and (C), we draw in Figure 9 the time series of $q_{1,t}$ in dark blue and of $q_{2,t}$ in green for

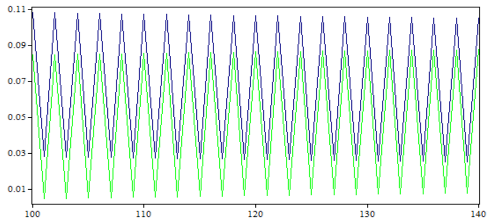

(A)

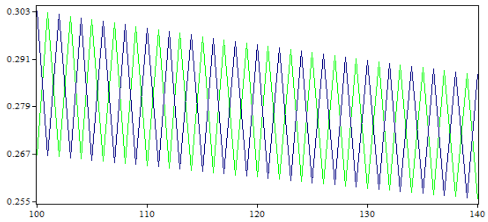

(B)

Figure 9: In (A) and (B) we show the time series of $q_{1,t}$ in dark blue and of $q_{2,t}$ in green for $t \in [101, 140]$, corresponding to the values of d marked in blue in Figure 8 (A) and (C), respectively.

$t \in [101, 140]$, corresponding to the values of d marked in blue in Figure 8 (A) and (C), i.e., $d = -0.477$ and $d = -0.468$, respectively. We find that, although for the considered values of d both the bifurcation diagrams of $q_{1,t+1}$ in Figures 4 (C) and 6 (B) highlight the presence of a stable period-two cycle, in Figure 9 (A) we witness an agreement between the periods of high/low production strategies for the two firms, so that their outputs give a concordant contribution to aggregate emissions in Figure 8 (A), while in Figure 9 (B) there is discordance between the high/low output choice timing for the two firms, still giving rise to a decreasing trend. Such difference between Figure 9 (A) and (B) is the reason why in the bifurcation diagram in Figure 8 (A) we witness a period-two cycle for U_{t+1} for low values for d, like it was in Figure 4 (C), while in Figure 8 (C) we do not see oscillations for U_{t+1} even before the stability threshold value, i.e., $d = -0.467$.
We stress that in the time series in Figure 9 (A) and (B) we introduced a transient of 100 periods in order to show the asymptotic behavior of the production of the two firms. We also remark that the choice of considering $T \in [0, 100]$ in our experiments in Figure 8 (B) and (D) has no effect on the behavior of time series for cumulative emissions. Namely, considering a larger time interval, the distance among the found time series would increase, but their ordering would not change. Moreover, we underline that the proposed technique can be applied to more general frameworks, in which looking at the corresponding bifurcation diagram with respect to d is not clear what is the effect generated by an increase in emission charges on produced quantities, and consequently on emissions.
Hence, thanks to our first method based on cumulative emissions we checked

in Figure 8 the efficacy of the environmental policy introduced in (2.2) for the parameter configurations considered in Subsection 3.1 and in Scenario I in Subsection 3.2, in agreement with the comparative statics results obtained for substitutes and complements under (3.15) in Propositions 1 and 4 in Naimzada and Pireddu (2023). In regard to Scenario II in Subsection 3.2, in which the Nash equilibrium is always unstable when it is admissible, we can say that if the system reached the steady state and remained on it despite the equilibrium instability, we would find that emissions raise with an increase in d, in agreement with Proposition 7 in Naimzada and Pireddu (2023), i.e., the comparative statics result valid for the case of complements under (3.16). On the other hand, since in Scenario II in Subsection 3.2 we are always in an instability regime and the numerical simulations we performed display divergent outcomes, with no emerging attractors, it is not possible to draw conclusions about the environmental policy efficacy in that scenario. Namely, related comments can be made just when orbits visit an attractor.
A different extension of the classical comparative statics analysis to the frameworks in which the steady state is not stable may lead to what we could call "comparative dynamics", consisting in a comparison, for the given parameter configuration and over a certain time interval, of cumulative emissions, starting from the unstable Nash equilibrium and from a different point in the basin of attraction of the stable periodic or complex attractor. We show what happens in this respect both with substitutes, in Figures 10 and 11, and with complements under (3.15), in Figures 12 and 13, starting in both cases from Figure 7 (C) and dealing with positive and negative values for γ, respectively.
Namely, in Figure 10 (A) we draw the bifurcation diagram of $q_{1,t+1}$ obtained for the same parameter values used in Figure 7 (C) but fixing $\gamma = 3$ and letting d vary in $(0.05, 0.15)$. Since the steady state (drawn in red, dashed line) is always unstable for the considered parameter values and, according to the value of $d \in (0.05, 0.15)$, we observe a periodic or a chaotic attractor (in blue), in order to perform a "comparative dynamics" exercise, we contrast in Figure 10 (B) the time series of cumulative emissions CE_T for $T \in [0, 100]$ corresponding to $d = 0.1$, with initial condition $u_{1,0} + u_{2,0} = \varepsilon(q_{1,0} + q_{2,0}) = 2.7 * 0.6 = 1.62$ for the blue points and $u_{1,0} + u_{2,0} = 2\varepsilon q_1^* = 2 * 2.7 * 0.139 = 0.751$ for the red points. We find that the cumulative emissions in the considered time interval are larger along the non-stationary trajectory than along the equilibrium path. Hence, we could try to contain emissions and to stabilize the system by acting on the sigmoid adjustment mechanism, and in particu-

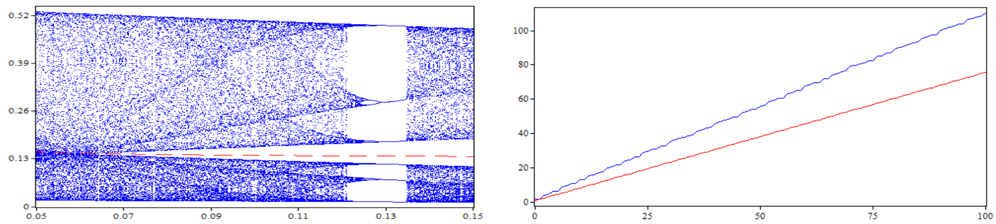

(A) (B)

Figure 10: In (A) the bifurcation diagram of $q_{1,t+1}$ in (3.1) with respect to $d \in (0.05, 0.15)$ with initial conditions $q_{1,0} = 0.1$, $q_{2,0} = 0.5$, for $p = 2.5$, $\delta = 0.4$, $\upsilon = 2.2$, $\beta = 3.1$, $c = 0.15$, $b = 0.4$, $\varepsilon = 2.7$, $\sigma = 6$ and $\gamma = 3$. In (B) we show the time series of cumulative emissions CE_T for $T \in [0, 100]$ corresponding to $d = 0.1$, with initial condition $u_{1,0} + u_{2,0} = 1.62$, connected with $q_{1,0} = 0.1$ and $q_{2,0} = 0.5$, for the blue points and $2\varepsilon q_1^* = 2 * 2.7 * 0.139 = 0.751$ for the red points.

lar on the position of its horizontal asymptotes. In this respect, we recall the bounding role played by the horizontal asymptotes, whose level, as explained in Section 2, is controlled by parameters υ and δ. Indeed, reducing υ lowers the upper asymptote, which plays a role when the best response is above the current production level, while decreasing δ raises the lower asymptote, which intervenes when the best response is below current production level. Starting from the framework in Figure 10 and acting for instance on υ, we obtain the effect illustrated in Figure 11, where in (A) and (C) we show that, as desired, the complexity of the dynamics decreases by lowering υ. In more detail, fixing the remaining parameters as in Figure 10 (A), in Figure 11 (A) for $\upsilon = 1.35$ we obtain a periodic attractor (in blue), i.e., a period-four or a period-two cycle for $d \in (0.05, 0.15)$, while the steady state (drawn in red, dashed line) is always unstable for such values of d. Drawing in Figure 11 (B) the time series of cumulative emissions for $T \in [0, 100]$ corresponding to $d = 0.1$, with initial condition $u_{1,0} + u_{2,0} = \varepsilon(q_{1,0} + q_{2,0}) = 2.7 * 0.6 = 1.62$ for the blue points and $u_{1,0} + u_{2,0} = 2\varepsilon q_1^* = 2 * 2.7 * 0.139 = 0.751$ for the red points, we find, like in Figure 10 (B), that cumulative emissions are larger along the non-stationary trajectory than along the equilibrium path. Reducing υ further to 0.5 in Figure 11 (C), we finally obtain the complete stabilization of the system. This shows that the sigmoid adjustment mechanism can be effective in reducing pollution, by acting on the maximum allowed produc-

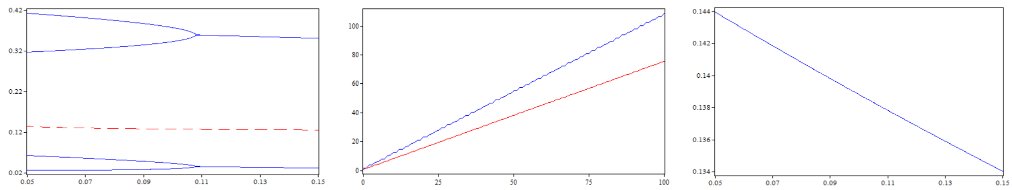

(A) (B) (C)

Figure 11: In (A) and (C) we report the bifurcation diagrams of $q_{1,t+1}$ in (3.1) with respect to $d \in (0.05, 0.15)$ with initial conditions $q_{1,0} = 0.1$, $q_{2,0} = 0.5$, for $p = 2.5$, $\delta = 0.4$, $\beta = 3.1$, $c = 0.15$, $b = 0.4$, $\varepsilon = 2.7$, $\sigma = 6$, $\gamma = 3$, and $\upsilon = 1.35$ in (A), $\upsilon = 0.5$ in (C), respectively. In (B) we show the time series of cumulative emissions CE_T for $T \in [0, 100]$ corresponding to (A) with $d = 0.1$, with initial conditions $u_{1,0} + u_{2,0} = 1.62$, connected with $q_{1,0} = 0.1$ and $q_{2,0} = 0.5$, for the blue points and $2\varepsilon q_1^* = 2 * 2.7 * 0.139 = 0.751$ for the red points.

tion variation. As argued above, in consequence of the system stabilization, the comparative statics analysis becomes economically grounded. We recall that, for the case of substitutes, the corresponding comparative statics result in Naimzada and Pireddu (2023) (cf. Proposition 1 therein) states that the equilibrium pollution level falls with an increase in emission charges. We stress that the outcome about the system stabilization is independent from the choice of considering $T \in [0, 100]$ in regard to the time frame, as well as from the choice of $d = 0.1$, since for any value of $d \in (0.05, 0.15)$ we would obtain the same conclusion, whether in Figure 10 (A) we observe a periodic or a chaotic attractor.
In fact, we shall reach analogous conclusions also with complements, when (3.15) holds true. In this case, starting again from Figure 7 (C), we draw in Figure 12 (A) the bifurcation diagram of $q_{1,t+1}$ obtained for the same parameter values used therein but fixing $\gamma = -3$ and letting d vary in $(0.05, 0.15)$, which highlights a multistability phenomenon. Since the steady state (drawn in red, dashed line) is always unstable for the considered parameter values and we observe two coexisting chaotic attractors (in blue and in green), interrupted just by some periodicity windows, in order to perform a comparative dynamics exercise, we contrast in Figure 12 (B) the time series of cumulative emissions CE_T for $T \in [0, 100]$ corresponding to $d = 0.1185$, with initial condition $u_{1,0} + u_{2,0} = \varepsilon(q_{1,0} + q_{2,0}) = 2.7 * 0.45 = 1.215$ for

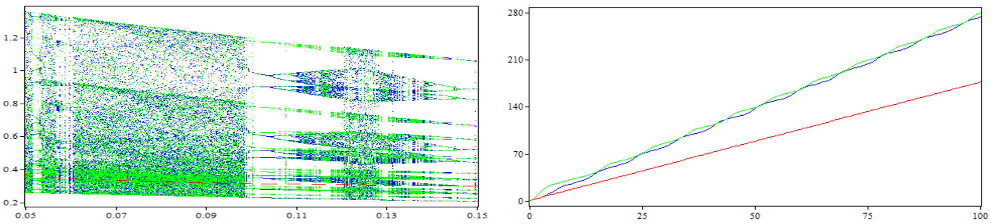

(A) (B)

Figure 12: In (A) the bifurcation diagram of $q_{1,t+1}$ in (3.1) with respect to $d \in (0.05, 0.15)$ with initial conditions $q_{1,0} = 0.25$, $q_{2,0} = 0.2$ for the blue points and $q_{1,0} = 0.1$, $q_{2,0} = 0.5$ for the green points, for $p = 2.5$, $\delta = 0.4$, $\upsilon = 2.2$, $\beta = 3.1$, $c = 0.15$, $b = 0.4$, $\varepsilon = 2.7$, $\sigma = 6$ and $\gamma = -3$. In (B) we show the time series of cumulative emissions CE_T for $T \in [0, 100]$ corresponding to $d = 0.1185$, with initial condition $u_{1,0} + u_{2,0} = 1.215$, connected with $q_{1,0} = 0.25$ and $q_{2,0} = 0.2$, for the blue points, $u_{1,0} + u_{2,0} = 1.62$, connected with $q_{1,0} = 0.1$ and $q_{2,0} = 0.5$, for the green points, and $2\varepsilon q_1^* = 2*2.7*0.325 = 1.757$ for the red points.

the blue points, $u_{1,0} + u_{2,0} = 2.7 * 0.6 = 1.62$ for the green points, and $u_{1,0} + u_{2,0} = 2\varepsilon q_1^* = 2 * 2.7 * 0.325 = 1.757$ for the red points. We find again that the cumulative emissions in the considered time interval are larger along the non-stationary trajectories than along the equilibrium path. Hence, also in this case we could try to contain emissions and to stabilize the system by acting on the sigmoid adjustment mechanism, and in particular by lowering the upper asymptote. Reducing υ we obtain the effect illustrated in Figure 13, where in (A) and (C) we show that, as desired, the complexity of the dynamics decreases when υ becomes smaller. In more detail, fixing the remaining parameters as in Figure 12 (A), in Figure 13 (A) for $\upsilon = 1.28$ we find (in blue) a quasiperiodic attractor in two pieces which loses stability in favor of a stable period-two cycle via a reverse Neimark-Sacker bifurcation for increasing values of $d \in (0.05, 0.15)$, while the steady state (in red, dashed line) is always unstable. Drawing in Figure 13 (B) the time series of cumulative emissions CE_T for $T \in [0, 100]$ corresponding to $d = 0.1$ with initial condition $u_{1,0} + u_{2,0} = \varepsilon(q_{1,0} + q_{2,0}) = 2.7 * 0.45 = 1.215$ for the blue points and $u_{1,0} + u_{2,0} = 2\varepsilon q_1^* = 2 * 2.7 * 0.336 = 1.814$ for the red points, we find that the cumulative emissions are larger along the quasiperiodic, non-stationary trajectory than on the Nash equilibrium. Lowering υ further to 0.5 in Figure

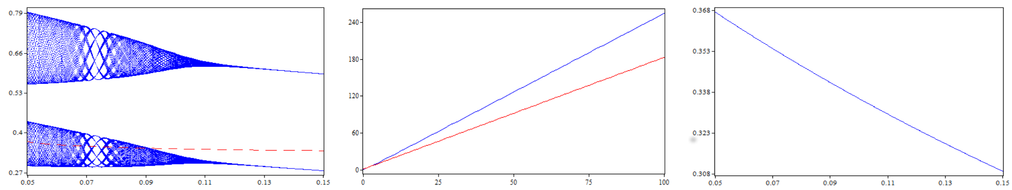

(A) (B) (C)

Figure 13: In (A) and (C) we report the bifurcation diagrams of $q_{1,t+1}$ in (3.1) with respect to $d \in (0.05, 0.15)$ with initial conditions $q_{1,0} = 0.25$, $q_{2,0} = 0.2$ for $p = 2.5$, $\delta = 0.4$, $\beta = 3.1$, $c = 0.15$, $b = 0.4$, $\varepsilon = 2.7$, $\sigma = 6$, $\gamma = -3$, and $\upsilon = 1.28$ in (A), $\upsilon = 0.5$ in (C), respectively. In (B) we show the time series of cumulative emissions CE_T for $T \in [0, 100]$ corresponding to (A) with $d = 0.1$, with initial conditions $u_{1,0} + u_{2,0} = 1.215$, connected with $q_{1,0} = 0.25$ and $q_{2,0} = 0.2$, for the blue points, and $2\varepsilon q_1^* = 2 * 2.7 * 0.336 = 1.814$ for the red points.

13 (C), we finally reach the stabilization of the system. This shows that the sigmoid adjustment mechanism is effective in reducing pollution, by acting on the maximum allowed production variation, also with complements under (3.15). Notice that such outcome is in agreement with the corresponding comparative statics result in Naimzada and Pireddu (2023) (cf. Proposition 4 therein), stating that the equilibrium pollution level falls with an increase in emission charges, which becomes economically grounded when υ is low enough, so that the steady state is stable. Again, the stabilization of the Nash equilibrium is independent from the choice of dealing with $T \in [0, 100]$ and $d \in (0.05, 0.15)$.

Summarizing, through our first method, based on a comparison of emissions for different levels of charges, we have found that increasing values for d raise the dynamic efficacy of the considered environmental policy, while the second approach, i.e., the "comparative dynamics" technique, has highlighted that, in order to reduce pollution, guaranteeing the convergence to the Nash equilibrium is preferable to allowing for complex or periodic behavior in the firms' output, and that acting on the asymptotes may correspond to a direct control of emissions, in contrast with the *indirect* nature of the pollution control obtained by means of the emission charges in (2.2). In this respect, we stress that the direct control exerted by acting on the sigmoid asymptotes stabilizes the Nash equilibrium without inducing any variation in the output level, contrary to the indirect control described by (2.2) which, according to Propositions 1 and 4 in Naimzada and Pireddu (2023), induces a negative variation in output. The above described conclusions have been reached for the parameter configurations considered in Section 3 both with substitutes and in Scenario I therein with complements under (3.15). On the other hand, due to the fact that, according to Proposition 3.3, the Nash equilibrium is never stable under (3.16) and that divergence issues arise in the numerical simulations we performed for Scenario II in Section 3, our techniques do not allow us to draw conclusions about the efficacy of the environmental policy when dealing with complements under (3.16).

5 Conclusion

In agreement with the results of the growing empirical and experimental literature (see e.g. Arango and Moxnes 2012; Chatrath et al. 2002; Gouel 2012; Huffaker et al. 2018), which highlights the chaotic behavior of the main variables involved in various markets, and in particular in agricultural commodity markets, we proposed a model able to generate interesting, erratic dynamic outcomes. In more detail, starting from the Cournot duopoly framework with quadratic emission charges and homogeneous goods in Mamada and Perrings (2020), we replaced the linear partial best response mechanism considered therein with a sigmoid adaptive best response mechanism, which, in addition to help avoid diverging trajectories and negativity issues, is also sensible from an economic viewpoint, being suitable to describe the gradual output variations caused by material, historical and institutional constraints in the production side of an economy, as well as by the limits imposed by an environmental policy scheme on production levels, due to their direct proportionality with emissions. Moreover, following the suggestion contained in the concluding section of Mamada and Perrings (2020), we assumed that firms produce differentiated goods. Beyond analytically studying the stability of the unique steady state, which coincides with the Nash equilibrium, and the effect produced by the main parameters on the stability region, we proposed two dynamical methods which allow to evaluate the environmental policy efficacy when the Nash equilibrium is not stable and thus the standard comparative statics approach does not fit for the purpose. Involving non-stationary orbits, the proposed techniques are mainly numerical in nature. In particular, the first technique, which is based on a comparison of emissions for different levels of charges, showed that, also when the Nash equilibrium is not stable, the considered environmental policy may be effective both with complements and substitutes. The second method, consisting in a comparison of emissions along non-stationary trajectories and along the equilibrium path, in the proposed experiments highlighted the presence of larger emissions along non-stationary trajectories. Hence, it gave us the opportunity to illustrate how an intervention on the sigmoid asymptotes may correspond to a direct control of emissions - in contrast with the indirect nature of the pollution control obtained by means of the considered emission charges - that also allows for a complete stabilization of the system, so that comparative statics results become economically grounded, starting from a situation characterized by the presence of a different attractor. In more detail, in making our numerical experiments, we have not only seen that the position of the asymptotes of the sigmoid is crucial in determining the system dynamics, but also that small variations in other parameters, such as the interdependence degree between goods, may generate important differences in the outcomes. In this respect we mention the work by Menueta et al. (2021), which suggests that a particularly careful choice of the (e.g. fiscal or environmental) policy to implement is needed when dealing with nonlinear models in which complex dynamics and bifurcation phenomena can emerge. We believe that the analyzed setting can be the starting point for other research works.

At first, we deem it essential to fully develop all dynamical aspects hidden inside the proposed model, in order to make it more realistic. Two possible extensions of the studied framework in such direction are represented respectively by the description of the environment as a sector interacting with the economic sphere and by the possibility of describing the transition among different market structures via an evolutive approach based on relative profitability of markets.

Regarding the former extension, in agreement with the seminal work by John and Pecchenino (1994), where the environment and its neglect are expressed through a dynamic equation, we could enrich the model by the introduction of one or more dynamic equations describing the evolution of the environment and its mutual interactions with the economic sector. In this manner, differently from the standard approach which depicts the environment in a parametric manner, it would be possible to deal with dynamical models consisting of coupled equations, in order to make explicit the effect of the economic activities on the evolution of the environment, as well as the impact of the environmental features on the economic activities, both in a direct manner, through consumption and production choices, and in an indirect way, through environmental policies. The addition of the dynamic equation(s) describing the environment evolution would make our "semi-dynamic" model fully dynamic and nonlinear. Usually, in that kind of models complex phenomena emerge, such as bifurcations, chaotic behavior, coexistence among different attractors. According to Costanza et al. (1993) and Perrings (1998), the environmental policy efficacy should be evaluated in those dynamic nonlinear models. In this respect, we stress that along the paper we measured the efficacy of the considered environmental policy in terms of its effectiveness in reducing emissions. Of course, a reduction in emissions is a consequence of an output decrease. A more general evaluation of an environmental policy scheme would require to deal with an oligopoly model that takes into account further variables, i.e., the factors of production, such as the employed labor (see e.g. Chiarella and Okuguchi, 1997).

In regard to the latter extension, concerning the transition among different market structures, we start by recalling that Mamada and Perrings (2020) tackle the issue of the market structure endogeneity, focusing in particular on the conditions that may lead from duopoly to monopoly, investigated also in Matsumoto et al. (2022) under the assumption that marginal production costs do not coincide across firms. An alternative approach to the problem of the market structure endogeneity could be evolutive in nature, with firms deciding whether to operate or not in a given market on the basis of a profitability signal, such as the comparison between the profitability of the market with respect to the average profitability of other markets. In this manner the number of firms operating in a market would become an endogenous variable. Such approach would allow to more generally investigate the conditions which lead, possibly in a reversible manner, from a market structure to another one.

Different extensions of the proposed framework, which would be useful in view of testing the robustness of the here obtained results, could concern the formulation of the demand functions of firms and their technology heterogeneity in regard to emissions. For instance, following Agliari et al. (2016), we might deal with demand functions deriving from an underlying CES utility function, while in relation to firms technology heterogeneity we recall that pollution abatement technologies not coinciding across firms have been considered e.g. in Ganguli and Raju (2012) and in Matsumoto et al. (2018b).

References

Agliari A, Naimzada AK, Pecora N (2016) Nonlinear dynamics of a Cournot duopoly game with differentiated products. Applied Mathematics and Computation 281, 1–15.

Arango S, Moxnes E (2012) Commodity cycles, a function of market complexity? Extending the cobweb experiment. Journal of Economic Behavior & Organization 84, 321–334.

Bischi GI, Chiarella C, Kopel M, Szidarovszky F (2010) Nonlinear Oligopolies. Stability and Bifurcations. Springer-Verlag, Berlin.

Bulow J, Geanakoplos J, Klemperer P (1985) Multimarket oligopoly: strategic substitutes and strategic complements. Journal of Political Economy 93, 488–511.

Chatrath A, Adrangi B, Dhanda KK (2002) Are commodity prices chaotic? Agricultural Economics 27, 123–137.

Chiarella C, Okuguchi, K (1997) A dynamic analysis of Cournot duopoly in imperfectly competitive product and factor markets. Keio Economic Studies 34, 21–33.

Costanza R, Wainger L, Folke C, Mäler K-G (1993) Modeling complex ecological economic systems. BioScience 43, 545–555.

Elaydi, SN (2007) Discrete Chaos: With Applications in Science and Engineering, 2nd Edition. Taylor & Francis Group, Boca Raton.

Ganguli S, Raju S (2012) Perverse environmental effects of ambient charges in a Bertrand duopoly. Journal of Environmental Economics and Policy 1, 1–8.

Gouel C (2012) Agricultural price instability: A survey of competing explanations and remedies. Journal of Economic Surveys 26, 129–156.

Huffaker R, Canavari M, Muñoz-Carpena R (2018) Distinguishing between endogenous and exogenous price volatility in food security assessment: An empirical nonlinear dynamics approach. Agricultural Systems 160, 98–109.

John A, Pecchenino R (1994) An overlapping generations model of growth and the environment. The Economic Journal 104, 1393–1410.

Jury EI (1964) Theory and Application of the z-Transform Method. John Wiley and Sons, New York.

Mamada R, Perrings C (2020) The effect of emission charges on output and emissions in dynamic Cournot duopoly. Economic Analysis and Policy 66, 370–380.

Matsumoto A, Nonaka Y, Szidarovszky F (2022) Emission charge controllability in Cournot duopoly: static and dynamic effects. Journal of Difference Equations and Applications 28, 1282–1307.

Matsumoto A, Szidarovszky F (2021) Controlling non-point source pollution in Cournot oligopolies with hyperbolic demand. SN Business & Economics 1, 38. DOI: 10.1007/s43546-020-00023-8

Matsumoto A, Szidarovszky F (2022) N-firm oligopolies with pollution control and random profits. Asia-Pacific Journal of Regional Science 6, 1017–1039.

Matsumoto A, Szidarovszky F, Takizawa H (2018a) Extended oligopolies with pollution penalties and rewards. Discrete Dynamics in Nature and Society 2018, Article ID 7861432, 8 pages.

Matsumoto A, Szidarovszky F, Yabuta M (2018b) Environmental effects of ambient charge in Cournot oligopoly. Journal of Environmental Economics and Policy 7, 41–56.

Menueta M, Minea A, Villieu P, Xepapadeas A (2021) Growth, endogenous environmental cycles, and indeterminacy. Working Paper Series, Economic Research Department of the University of Orléans, DR LEO 2021-10

Motta, M (2004) Competition Policy: Theory and Practice. Cambridge University Press, Cambridge.

Naimzada A, Pireddu M (2014) Dynamic behavior of product and stock markets with a varying degree of interaction. Economic Modelling 41, 191–197.

Naimzada A, Pireddu M (2015) Introducing a price variation limiter mechanism into a behavioral financial market model. Chaos: An Interdisciplinary Journal of Nonlinear Science 25, 083112.

Naimzada A, Pireddu M (2023) Differentiated goods in a dynamic Cournot duopoly with emission charges on output. Decisions in Economics and Finance. DOI: 10.1007/s10203-023-00387-0

Perrings C (1998) Resilience in the dynamics of economy-environment systems. Environmental and Resource Economics 11, 503–520.

Raju S, Ganguli S (2013) Strategic firm interaction, returns to scale, environmental regulation and ambient charges in a Cournot duopoly. Technology and Investment 4, 113–122.

Sarafopoulos G, Papadopoulos K (2017) On a Cournot duopoly game with differentiated goods, heterogeneous expectations and a cost function including emission costs. Scientific Bulletin - Economic Sciences 16, 11–22.

Sato H (2017) Pollution from Cournot duopoly industry and the effect of ambient charges. Journal of Environmental Economics and Policy 6, 305–308.

Singh N, Vives X (1984) Price and quantity competition in a differentiated duopoly. Rand Journal of Economics 15, 546–554.

Stanley C (2020) Living to spend another day: Exploring resilience as a new fourth goal of ecological economics. Ecological Economics 178, 106805.